ANNUAL REVIEWS

Annual Review of Earth and Planetary Sciences

Past Warmth and Its Impacts During the Holocene Thermal Maximum in Greenland

Yarrow Axford,[1] Anne de Vernal,[2] and Erich C. Osterberg[3]

[1]Department of Earth and Planetary Sciences, Northwestern University, Evanston, Illinois 60201, USA; email: axford@northwestern.edu

[2]Geotop Research Center and Department of Earth and Atmospheric Sciences, Université du Québec à Montréal, Montréal, Québec H3C 3P8, Canada

[3]Department of Earth Sciences, Dartmouth College, Hanover, New Hampshire 03755, USA

Annu. Rev. Earth Planet. Sci. 2021. 49:279–307

First published as a Review in Advance on December 21, 2020

The *Annual Review of Earth and Planetary Sciences* is online at earth.annualreviews.org

https://doi.org/10.1146/annurev-earth-081420-063858

Keywords

Arctic, Holocene Thermal Maximum, Greenland Ice Sheet, paleoclimate, paleoceanography, paleolimnology

Abstract

Higher boreal summer insolation in the early to middle Holocene drove thousands of years of summer warming across the Arctic. Modern-day warming has distinctly different causes, but geologic data from this past warm period hold lessons for the future. We compile Holocene temperature reconstructions from ice, lake, and marine cores around Greenland, where summer temperatures are globally important due to their influence on ice sheet mass balance, ocean circulation, and sea ice. Highlighting and accounting for some key issues with proxy interpretation, we find that much of Greenland experienced summers 3 to 5°C warmer than the mid-twentieth century in the early Holocene—earlier and stronger warming than often presumed. Warmth had dramatic consequences: Many glaciers disappeared, perennial sea ice retreated, plants and animals migrated northward, the Greenland Ice Sheet shrank rapidly, and increased meltwater discharge led to strong marine water stratification and enhanced winter sea ice in some areas.

- Summer air temperatures and open ocean temperatures around much of Greenland peaked in the early Holocene in response to elevated summer insolation.
- Peak summer air temperatures ranged from 3 to 5°C warmer than the mid-twentieth century in northwest and central Greenland to perhaps 1 to 2°C warmer in south Greenland.
- Many differences between records can be explained by proxy seasonality, ice sheet elevation changes, vegetation analogs and lags, and the nearshore effects of ice sheet meltwater.
- Early Holocene warmth dramatically affected glaciers and the Greenland Ice Sheet; meltwater discharge, nearshore ocean salinity, and sea ice; and diverse flora and fauna.

1. INTRODUCTION

Warming climate in recent decades has had wide-ranging effects on Greenland's environment, from shrinking sea ice and glaciers to changing marine mammal behavior, plant phenology, and caribou calving (Kerby & Post 2013, Meier et al. 2014). In a recent survey, three out of four Greenland residents reported personally experiencing effects of climate change (Minor et al. 2019). The Greenland Ice Sheet has been rapidly losing mass since the 1990s (Mouginot et al. 2019). If we do not limit future global warming, the ice sheet appears destined for eventual disappearance, with a consequent ~7-m global sea level rise (Clark et al. 2016). Rates of future ice sheet loss are highly uncertain.

Here we review geologic data from the most recent and best-studied past period of protracted temperatures warmer than the mid-twentieth century AD over Greenland (**Figure 1*a–d***): the Holocene Thermal Maximum (HTM) in the early to middle Holocene. Our subdivision of the Holocene follows Walker et al. (2018), with the early, middle, and late Holocene beginning at 11.7, 8.2, and 4.2 ka, respectively (with ka meaning thousands of years before 1950 AD). It has long been recognized that Greenland and much of the Arctic experienced temperatures warmer than today during part of the Holocene, in response to slow, predictable changes in summer insolation. The dramatic impacts of HTM warming around Greenland contrast with the canonical view of stable Holocene climate. Marine species in Baffin Bay migrated 1,000 km north, and trees and shrubs advanced northward of their current ranges (Kaufman 2004). Many of today's ice caps and mountain glaciers were smaller or nonexistent (Kelly & Lowell 2009, Larocca et al. 2020a, Larsen et al. 2019), and the Greenland Ice Sheet shrank smaller than it is today (Larsen et al. 2015, Young & Briner 2015). Perennial sea ice retreated perhaps 1,000 km from its modern edge north of Greenland (Funder et al. 2011). HTM warming was driven primarily by astronomical forcing, which today exerts a cooling influence on the Northern Hemisphere that has been demonstrably overwhelmed by anthropogenic greenhouse gas forcing (Kaufman et al. 2009). Despite these different drivers of warmth, the HTM provides unique insights into the dynamics and impacts of long-term warming and is therefore highly relevant to understanding future climate change.

Historically, estimates of the timing of peak HTM warmth in Greenland have differed by thousands of years, and reconstructions of its magnitude have varied by several degrees, confounding our understanding of how temperature changes affect the ice sheet, ecosystems, and ocean conditions (e.g., Badgeley et al. 2020, Briner et al. 2016, Gajewski 2015b, McFarlin et al. 2018). In the past decade new approaches to estimating paleotemperatures from ice cores, quantitative methods applied to lake and marine sediment cores, and numerous glacial geologic studies together have enhanced our knowledge of Holocene climate change. We summarize the resulting overall picture, with a focus on reconstructions of multimillennial trends in air and sea-surface temperatures (SSTs)—climate variables with pervasive influence on Greenland's environment (for an overview of relevant paleoclimate reconstruction methods, see **Table 1**). We first evaluate and synthesize

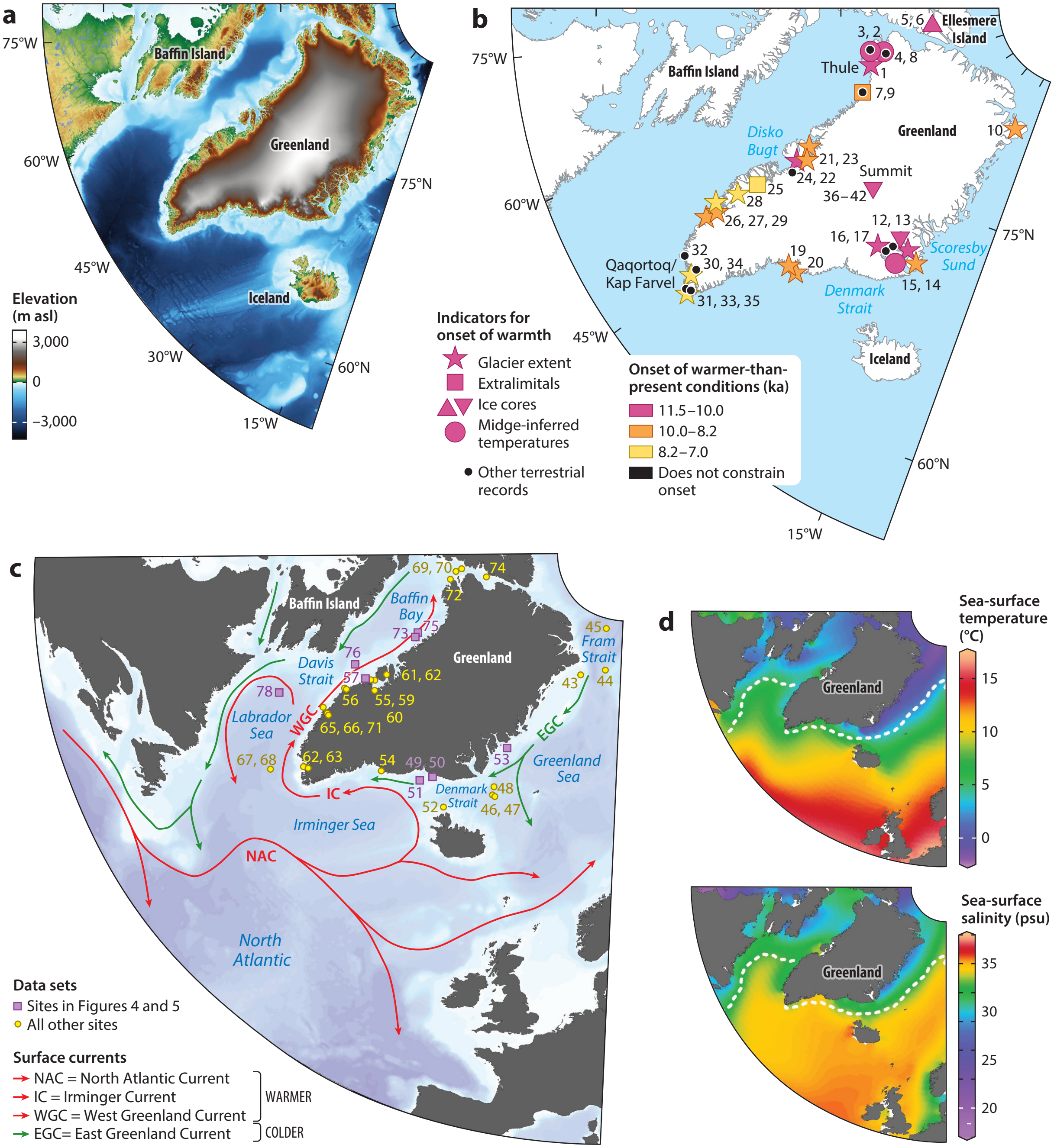

(Caption appears on following page)

Figure 1 (*Figure appears on preceding page*)

(*a*) Topographic and bathymetric features of Greenland and surrounding seas. (*b*) Climate reconstruction sites mentioned in the text and **Figures 2** and **3**; the numbers in parentheses refer to the code numbers in **Supplemental Table 1**. Sites with colored symbols provide robust indicators for the onset of summers warmer than in the mid-twentieth century AD, based on mountain glaciers and ice caps smaller than today, extralimital terrestrial taxa, melt at Agassiz Ice Cap (*upright triangle*) and midge-inferred temperatures. Inverted triangles are annual proxies from ice cores. Other records (*black circles*) include pollen-inferred summer temperatures, which we find are often affected by migration lags or no-analog conditions in the early Holocene; and midge- and isotope-inferred summer temperature records that do not extend to the early Holocene. (*c*) Northern North Atlantic with main surface currents and locations of data sets in **Supplemental Table 1** and **Figures 4** and **5**. (*d*) Modern summer sea-surface temperature and sea-surface salinity (data from NCEI 2009) and median maximum winter sea-ice extent (*dashed white lines*) (data from Natl. Snow Ice Data Cent. 2020).

Supplemental Material >

records from land (ice cores, followed by and compared with lake sediments) (**Figure 1*b***) and then summarize key marine records (**Figure 1*c***), contrasting nearshore versus offshore environments. From this diverse mix of evidence, we summarize multimillennial temperature trends across Greenland. We also note caveats for interpreting some archives and proxies as indicators of regional climate, and we highlight priorities for future research.

2. HOLOCENE THERMAL MAXIMUM TEMPERATURES OVER LAND

2.1. Traditional and Updated Views from Ice Cores

Until about a decade ago, the only continuous quantitative reconstructions of air temperatures over Greenland came from ice cores. Ice core temperature reconstructions are based upon stable isotopes of ice (δD or δ^{18}O), prevalence of melt layers, borehole temperatures, and most recently isotopes of nitrogen (δ^{15}N) and/or argon (δ^{40}Ar) in trapped air (**Table 1**). Stable water isotopes provide an annual average vapor condensation temperature biased by the seasonal distribution of snowfall, whereas borehole temperatures, δ^{15}N, and δ^{40}Ar provide mean annual surface ice temperatures, and melt layers provide a summer temperature signal. Perhaps the most accurate ice core temperature histories come from δ^{15}N and δ^{40}Ar records because they are not biased by seasonal signals, they have multidecadal resolution, and the proxy is based on the relatively well-constrained physics of thermal fractionation in firn (Buizert et al. 2018, Kobashi et al. 2017). Holocene temperature records based on ice core stable isotopes have high resolution (often subannual) but require assumptions about the relationship between surface temperature (T_s) and δD (δ^2H) or δ^{18}O through time. This relationship is sensitive to a number of complex variables including changes in air mass trajectories, moisture sources, and precipitation seasonality (Dansgaard 1961). At Summit on the central ice sheet (**Figure 1**), borehole temperatures have been used to calibrate δ^{18}O-T_s (Cuffey & Clow 1997, Johnsen et al. 1995), and therefore borehole and stable isotope records of peak Holocene warmth are not fully independent. Hereafter, we discuss δ^{18}O records, but the results are essentially the same for δD.

Ice core and borehole temperature reconstructions from Summit [Greenland Ice Core Project (GRIP) and GISP2] are often employed to represent Greenland-wide temperature trends. When not corrected for ice sheet surface elevation changes (see discussion of elevation in Section 2.1.2) (**Figure 2*a***), Summit δ^{15}N and δ^{40}Ar records indicate peak annual average temperatures at the ice sheet surface 0.5–2.0°C warmer than the mid-twentieth century (defined here for all ice core records as the 1930–1970 mean) from 9.5 to 6.5 ka, interrupted by the cold 8.2 ka event (Buizert et al. 2018, Kobashi et al. 2017) (**Figure 2*b***). Oxygen isotope records from Summit are nearly trendless over the early–middle Holocene but show multidecadal periods of stronger warmth from ~10 to 6.5 ka broadly similar to the Summit δ^{15}N and δ^{40}Ar data (Johnsen et al. 2001, Masson-Delmotte et al. 2005) (**Figure 2*c***). In contrast, a recent paleoclimate data assimilation based on stable isotope records across Greenland found a +1–2°C HTM anomaly centered ~5 ka,

Table 1 Brief descriptions of paleoclimate proxies used in this review

Proxy method	Archive	Reconstructed variable(s)	Underlying principle
Midge assemblages	Lake sediment	Summer air temperature	Modern arctic insect (chironomid midge) species distributions are strongly correlated with summer temperatures.
Oxygen isotopes of midges	Lake sediment	Air temperature (from stable isotopes of precipitation)	Aquatic insect larval remains capture oxygen isotopic composition of lakewater (thus, at some sites, precipitation).
Pollen assemblages	Lake sediment	Summer air temperature	Modern arctic plant species distributions are strongly correlated with summer temperatures.
Glacier-fed lake	Lake sediment	Presence/absence or extent of glacier ice	When present in lakes' watersheds, glaciers supply distinct minerogenic sediments to lakes.
Extralimital species	Lake sediment	Warmer-than-modern temperature	Macro-remains of fish and invertebrates preserved north of their modern-day ranges record warmer past climate.
Melt stratigraphy	Ice	Summer air temperature	Warmer temperatures cause surface melt preserved as refrozen layers on ice caps and the Greenland Ice Sheet.
Borehole temperatures	Ice	Annual air temperature	Inverse modeling of temperatures measured in ice core boreholes yields smoothed estimates of past temperatures.
Oxygen and deuterium isotopes of ice	Ice	Annual (precipitation-biased) air temperature	Condensation temperature is a major control on stable isotopes of precipitation.
Nitrogen and argon isotopes	Ice	Annual air temperature	Temperature gradients in the firn column drive fractionation of nitrogen and argon gas, which is then preserved in ice bubbles.
IP_{25} biomarker	Marine sediment	Sea-ice conditions	Ice-dwelling diatoms are the only known source of a compound dubbed IP_{25} (an isoprenoid with 25 carbon atoms).
Diatom assemblages	Marine sediment	Sea-surface temperatures, sea-ice conditions	Modern assemblages of marine diatom algae relate to sea-surface temperatures and other surface water parameters.
Dinocyst assemblages	Marine sediment	Sea-surface temperature, salinity, sea-ice conditions	Modern dinoflagellate species distributions relate to sea-surface temperatures and salinity, and seasonal ice cover.
Planktic foraminiferal assemblages	Marine sediment	Surface to subsurface ocean temperatures	Modern assemblages of calcareous planktonic foraminifers relate to temperatures in the upper water column.
Benthic foraminiferal assemblages	Marine sediment	Ocean bottom water conditions	Modern assemblages of benthic foraminifers relate to environmental conditions on the seafloor.
Magnesium/calcium in foraminifers	Marine sediment	Water temperature	Temperature controls Mg:Ca ratio in calcium carbonate precipitated when foraminifers form their shells.
Alkenones	Marine sediment	Surface temperature	In cultures and core tops, temperature predicts unsaturation of alkenone lipids produced by marine haptophyte algae.

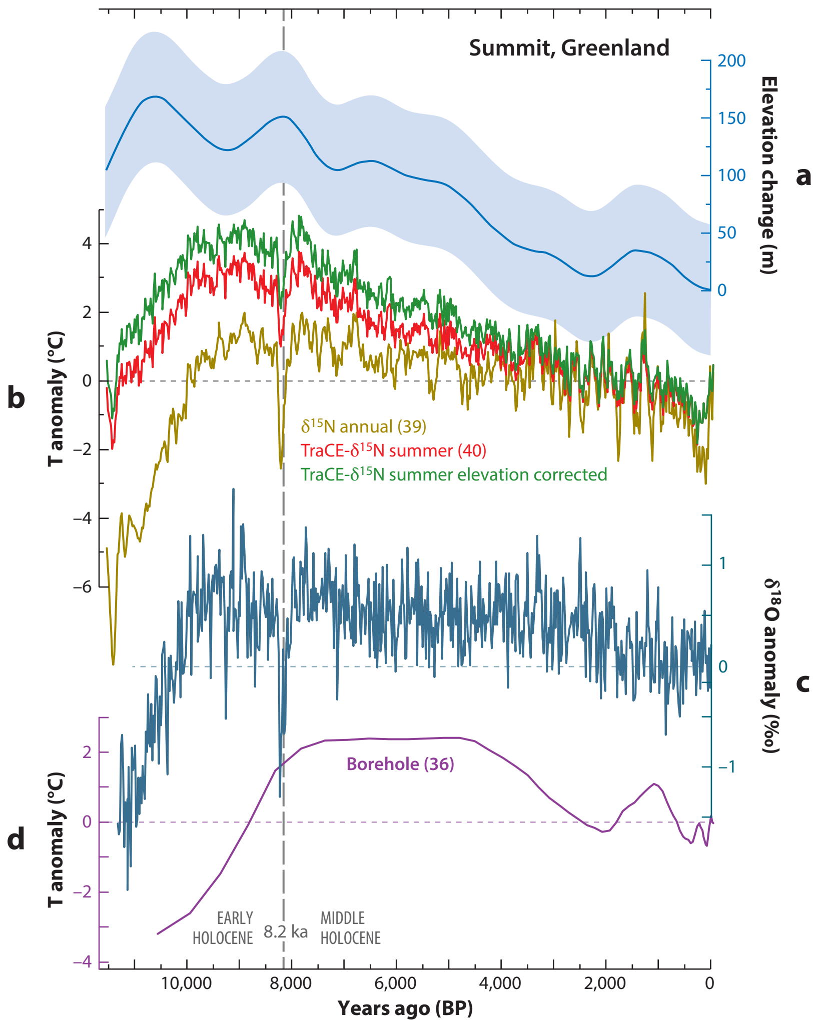

Figure 2

Evidence from ice cores including (*a*) estimated surface elevation change at Summit (*dark blue*) (Vinther et al. 2009) and uncertainty (*faded blue shading*) (Lecavalier et al. 2013), (*b*) annual $\delta^{15}N$ (*dark yellow*) and summer (*red*) and elevation-corrected summer (*green*) Summit temperature anomalies from TraCE-$\delta^{15}N$ (Buizert et al. 2018), (*c*) Greenland Ice Core Project (GRIP) oxygen isotopes (Rasmussen et al. 2006, Vinther et al. 2006), and (*d*) GRIP borehole temperature reconstruction (Dahl-Jensen et al. 1998). The vertical dashed line marks the boundary between early and middle Holocene at 8.2 ka. The numbers in parentheses refer to the code numbers in **Figure 1*b*** and **Supplemental Table 1**. All proxies are shown as anomalies relative to the 1930–1970 mean.

Supplemental Material >

considerably later than other ice core interpretations (Badgeley et al. 2020). However, this reconstruction is influenced by the large ice sheet surface elevation lowering at sites closer to the ice sheet margin [i.e., Camp Century and Dye-3 (Vinther et al. 2009)] during the first half of the Holocene, when local temperatures at the ice sheet surface were depressed by higher surface elevation. Despite having a later (~5 ka) peak in Holocene warmth than Summit $\delta^{15}N$ and $\delta^{40}Ar$ records, the assimilation-based reconstruction shows HTM temperatures exceeding those of the mid-twentieth century by 8 ka. Borehole paleothermometry indicates warmer-than-modern temperatures by 8.5 ka and mean annual HTM temperature anomalies of +2.4°C from ~7.5 to 4.5 ka (**Figure 2*d***); notably, this method has lower resolution than $\delta^{15}N$, $\delta^{40}Ar$, and $\delta^{18}O$.

Ice core paleotemperature reconstructions from the independent Agassiz (**Figure 3*a***) and Renland (**Figure 3*b***) Ice Caps [on Ellesmere Island, Canada, and in central east Greenland, respectively (see **Figure 1*b*** for locations)] are more representative of coastal Greenland temperatures and have been corrected for estimated changes in ice surface elevation arising from regional isostasy and changes in ice cap thickness. The elevation-corrected Renland stable isotope temperature reconstruction (Vinther et al. 2009) shows early Holocene peak warmth from ~9.5 to 7.5 ka, with a long-term cooling trend over the Holocene (**Figure 3*b***). The Agassiz Ice Cap stable isotope and melt layer temperature reconstructions differ significantly in the earliest Holocene from those at Summit and Renland, with an even earlier (~11–8 ka) and warmer (+3–5.5°C mean annual; +0.5–4°C summer) HTM at Agassiz (Lecavalier et al. 2017) (**Figure 3*a***). The warmer Agassiz stable isotope temperatures from 11 to 9 ka arise only after correcting for rather uncertain changes in Innuitian Ice Cap elevation, but the Agassiz record largely matches Renland temperature anomalies from 9 ka to present when ice elevation changes are better constrained (Lecavalier et al. 2017, Vinther et al. 2009).

2.1.1. Accounting for seasonality.

Summer air temperatures control many key elements of the Arctic system, including ice sheet surface melt, and as such should be high-priority targets for paleoclimate reconstructions. However, evidence for summer conditions over the Greenland Ice Sheet itself is sparse. Summit melt layers indicate peak summer warmth from 8 to 6 ka, but the magnitude of warming is uncertain from this record (Alley & Anandakrishnan 1995). Alley & Anandakrishnan (1995) also report lower confidence in the melt record prior to 8 ka due to clathrates in the ice; thus, the melt layer record does not preclude earlier summer warmth at Summit. Buizert et al. (2018) merged the transient Community Climate System Model version 3 (CCSM3) run from 21 ka to present (Liu et al. 2009) with the Summit $\delta^{15}N$ ice core record (hereafter TraCE-$\delta^{15}N$) to develop seasonal temperature reconstructions across Greenland. In this reconstruction, the timing and magnitude of annual mean temperature changes are constrained by the Summit $\delta^{15}N$ record, whereas their seasonality and spatial pattern are generated by the climate model (Buizert et al. 2018). At Summit, the TraCE-$\delta^{15}N$ summer temperature reconstruction peaks at +2.5–3.75°C from ~10 to 7 ka, 2–2.5°C warmer than the mean annual reconstruction from $\delta^{15}N$ and $\delta^{40}Ar$ (Buizert et al. 2018, Kobashi et al. 2017) (**Figure 2*b***).

In general, the TraCE-$\delta^{15}N$ reconstructions suggest that the HTM in Greenland was most pronounced in summer, with no long-term trend in wintertime temperatures from ~9 to 1 ka. Pronounced early Holocene summer warmth in the TraCE-$\delta^{15}N$ reconstruction is driven by strong early Holocene insolation forcing in CCSM3, whereas winter temperatures are more sensitive to the relatively muted changes in greenhouse gas forcing and overturning circulation (Buizert et al. 2018). Annual temperature reconstructions—such as those from ice core $\delta^{18}O$, $\delta^{15}N$, and borehole records—would therefore be expected to show a more muted and perhaps later HTM.

To improve understanding of past summer temperatures over the ice sheet, there is a need for additional summer-specific proxies from ice cores. Melt layers indicate summer warmth but can be difficult to interpret in the early Holocene because clathrate formation reduces the bubbles in ice cores that are used to identify melt (Alley & Anandakrishnan 1995). Techniques to more confidently interpret melt layers in the clathrate brittle zone are needed. Another challenge with Greenland melt layer records is that melt occurs infrequently in the dry snow zone. Despite 2.7°C warming at Summit from 1982 to 2011 (McGrath et al. 2013), only two summer melt events have occurred since 1889 (in 2012 and 2019) (Nghiem et al. 2012). Collecting early Holocene ice cores from lower-elevation sites on the ice sheet where melt is more common, but still infrequent

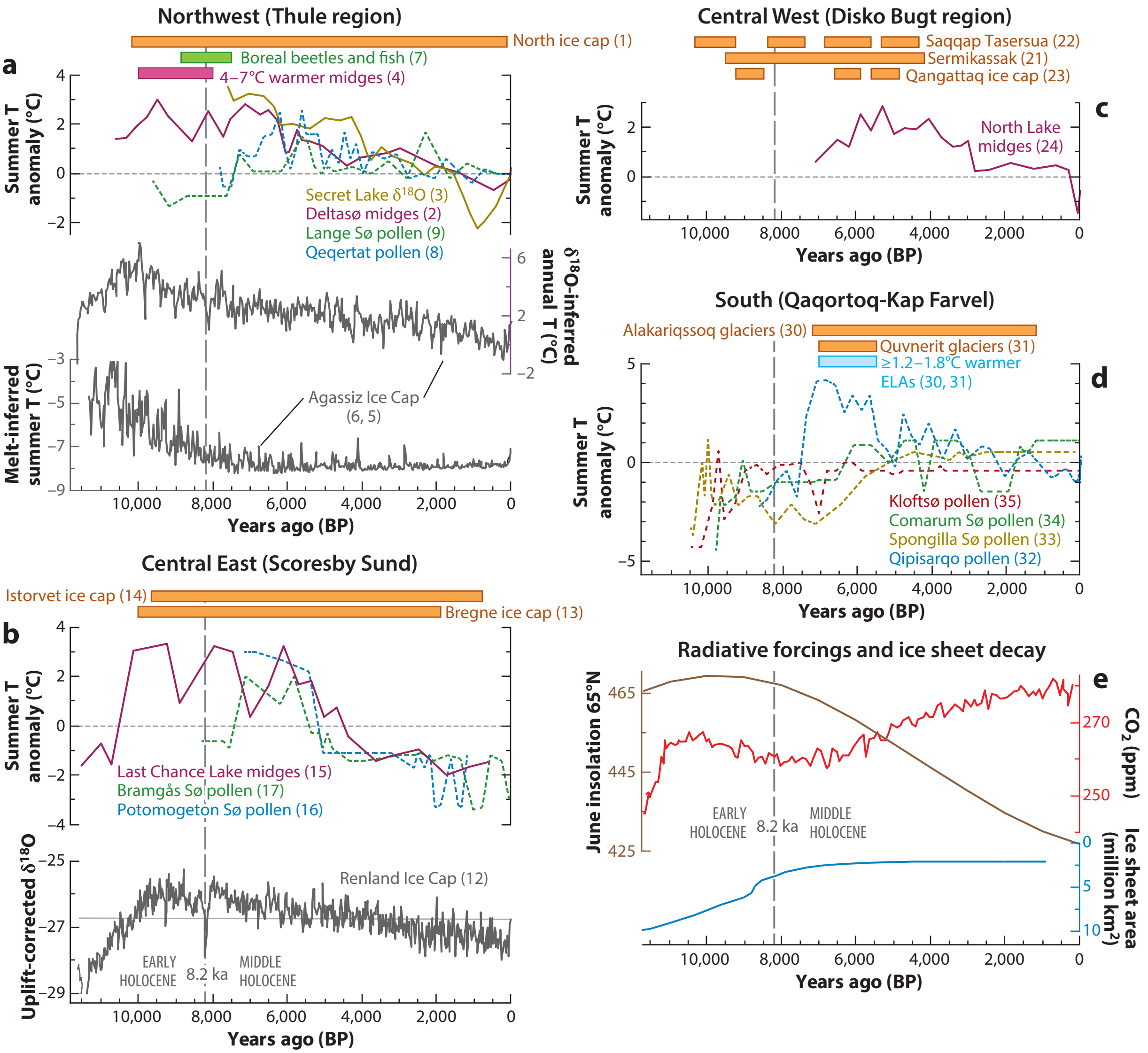

Figure 3

(*a–d*) Holocene air temperature indicators. Colored bars show qualitative indicators of summers warmer than the mid-twentieth century AD (smaller-than-present mountain glaciers and ice caps in *orange*; northward migrations of terrestrial species in *green*) and discontinuous quantitative estimates (*red*) from midge assemblages and reconstructed glacier equilibrium line altitudes (ELAs) (*light blue*). Colored curves show summer temperature anomalies relative to the mid-twentieth century. Gray curves show data from large marginal ice caps. δ^{18}O from ice cores is an annual proxy. Note the divergence between pollen-based reconstructions (*dashed data curves*) and other indicators in the early Holocene, whereas all indicators largely agree through the middle and late Holocene. The numbers in parentheses refer to the code numbers in **Figure 1*b*** and **Supplemental Table 1**. (*e*) Climate forcings and influences including June insolation (Berger & Loutre 1991), atmospheric CO_2 (Monnin et al. 2004), and decline of the Laurentide-Innuitian-Cordilleran ice sheet complex (Dalton et al. 2020, *y*-axis reversed).

Supplemental Material >

enough to preserve glaciochemical records (Graeter et al. 2018), may prove beneficial. As we discuss in Section 2.1.2, however, elevation corrections are critical and become even more important closer to the ice sheet margin where early Holocene elevation changes approach 1 km (Lecavalier et al. 2017).

2.1.2. Accounting for ice sheet surface elevation changes. Ice core temperature reconstructions are affected by changes in ice sheet surface elevation caused by isostasy and changes in ice sheet thickness. Changes in ice sheet surface elevation are poorly constrained in the Holocene but likely range from ∼150 m at Summit to ∼1,000 m closer to the ice sheet margins at sites such as Camp Century (Lecavalier et al. 2017). Ice sheet elevation peaked in the early Holocene when Summit snow accumulation rates tripled coming out of the Younger Dryas, and subsequently elevation generally declined toward present (Cuffey & Clow 1997, Dahl-Jensen et al. 1998, Lecavalier et al. 2017, Vinther et al. 2009) (**Figure 2*a***). Consequently, early Holocene ice core paleotemperature reconstructions appear cooler than they would if the ice sheet surface had maintained constant elevation throughout the Holocene, resulting in a muted early Holocene HTM signal in ice cores. Most ice core–based temperature records have not been corrected for elevation changes, in part because past elevation changes remain uncertain prior to 8 ka and especially in the late Pleistocene (Lecavalier et al. 2013). As a result, most reconstruct temperatures at nonconstant elevation.

To estimate the effect of elevation changes on Holocene temperature reconstructions, we apply the estimate of Summit surface elevation change (165 m of elevation decline since 10.5 ka) (**Figure 2*a***) by Vinther (2009) and a seasonally invariant lapse rate of 7.5°C/km (Ohmura 1987). These elevation estimates were revised from 0 to 8 ka by Lecavalier et al. (2013), but the corrections at Summit were minimal and we adopt the larger uncertainty bounds by Lecavalier et al. (2013) in **Figure 2**. Uncertainty is greater prior to 8 ka (Lecavalier et al. 2013), and evidence indicates that Summit elevation was higher in the early Holocene than in the middle Holocene (Cuffey & Clow 1997, Dahl-Jensen et al. 1998, Vinther et al. 2009). Our objective here is to demonstrate the importance of elevation on ice core temperature reconstructions; a more rigorous analysis of Summit elevation is beyond the scope of this review.

After correcting for elevation in this way, we find that Summit ice core temperatures shift ∼0.8–1.2°C warmer relative to the original records from 11 to 6 ka (**Figure 2*b***). Annual average Summit temperature anomalies from δ^{15}N and δ^{40}Ar records shift to +2–2.5°C from ∼9.5 to 6.5 ka, and summertime Summit temperature anomalies from the TraCE-δ^{15}N (Buizert et al. 2018) reconstruction shift to +3.5–4.75°C from ∼10 to 7 ka (**Figure 2*b***). Thus, accounting for both seasonality and elevation change yields a summertime HTM at Summit ∼2.5–3.25°C warmer in the early Holocene than conventionally inferred from annual average estimates without elevation correction. Furthermore, elevation corrections produce peak warmth over the central ice sheet in the early rather than middle Holocene.

2.2. The Summer-Focused View from Lakes

Beyond the limited summer perspective from ice cores described above, most summer air temperature reconstructions for Greenland come from lake sediments. Lake records have long been used to infer environmental and climatic change in Greenland (e.g., Fredskild 1985, Funder 1978, Iversen 1952). Recently paleolimnologists have applied quantitative methods to reconstructing Greenland temperatures (see **Table 1** for an overview of methods; see **Figures 1** and **3** and **Supplemental Table 1** for specific sites and records; see **Supplemental References** for literature cited in the supplemental table). Although data coverage for Greenland is sparse overall, several regions now have long-term (≥7 kyr) quantitative reconstructions of summer air temperatures based

Supplemental Material >

upon multiple methods and sites: the northwest (Thule region), central east (Scoresby Sund), central west (Disko Bugt region), and far south (Qaqortoq-Kap Farvel). Continuous, quantitative summer air temperature reconstructions in these regions come from pollen (Fréchette & de Vernal 2009; Gajewski 2015b, based upon earlier pollen stratigraphic analyses, e.g., by Fredskild 1985) (see **Supplemental Table 1**), midge assemblages [Diptera: Chironomidae (Axford et al. 2013, 2017, 2019)], melt on the Agassiz Ice Cap (discussed in Section 2.1) (Lecavalier et al. 2017), and a record of precipitation isotopes inferred from $\delta^{18}O$ of aquatic midge larval head capsules in lake sediments (Lasher et al. 2017). In addition, lakes can capture continuous records of glaciofluvial sediment flux from glaciers within their watersheds, commonly expressed as onset (or end) of inorganic, minerogenic sedimentation when a glacier forms in the watershed (or disappears). Such lake sediment records of local ice cap and mountain glacier fluctuations provide complementary qualitative indicators of summer temperatures (Balascio et al. 2015; Larocca et al. 2020a,b; Larsen et al. 2017; Levy et al. 2014; Lowell et al. 2013; Schweinsberg et al. 2017, 2018, 2019; van der Bilt et al. 2018). So do occurrences of extralimital land plants and invertebrates that temporarily migrated northward during warmer periods (Bennike et al. 2010, Fredskild 1985, Funder 1978).

Supplemental Material >

We highlight multiproxy comparisons rather than individual records because each proxy method has its own unique strengths and limitations. For midge assemblages, an appropriate modern training set with good analogs for fossil assemblages must be available, and without careful site selection strong secondary gradients (for example, arising from changes in trophic status or lakewater oxygenation) may confound temperature signals as watersheds evolved through the Holocene (e.g., Brodersen & Anderson 2002). Relationships between precipitation isotopes and air temperatures shift over space and time with changing physiography and climate. It takes time for glacier extents to reach equilibrium with climate, and glacier mass balance may also be affected by any large changes in snowfall. Possible problems with pollen-based temperature reconstructions are discussed in the next section. By design, our summary of multiproxy comparisons excludes several pollen-based reconstructions from regions where no independent proxies have been analyzed for comparison. Because we use lakes to quantify summer air temperatures, for consistency we do not include lake records that offer qualitative or annual temperature reconstructions or that reconstruct lakewater temperatures (e.g., D'Andrea et al. 2011; Gajewski 2015b; Lasher et al. 2020; Schmidt et al. 2011; Thomas et al. 2016, 2018; von Gunten et al. 2012; Wooller et al. 2004).

2.2.1. On pollen-inferred temperatures. The majority of quantitative summer temperature reconstructions in Greenland [and Arctic-wide; (Kaufman et al. 2020)] come from pollen. Pollen is extensively calibrated as a surface air temperature proxy (Fréchette et al. 2008, Gajewski 2015b). Complications may arise from the potential for novel plant communities that occurred in ancient climates lacking modern analogs (e.g., due to enhanced early Holocene seasonality or altered precipitation regimes) and climate-vegetation lags due to the gradual march of postglacial species migration. These effects have long been debated. Gajewski (2015a) found that time since local deglaciation did not predict abundances of most plant types in Holocene pollen spectra across the Canadian archipelago and Greenland. However, sedimentary plant DNA revealed long vegetation lags in the early Holocene at a Baffin Island lake (Crump et al. 2019). Early Holocene vegetation structure with no modern analog has been extensively documented in Beringia (Edwards et al. 2005).

We find that in the three regions of Greenland where long-term pollen records can be compared with independent evidence for summer temperatures, the majority of pollen records diverge from other proxies when the latter indicate peak warmth in the early Holocene. Most pollen-inferred summer temperature reconstructions rose above mid-twentieth-century values centuries to millennia after nearby glaciers shrank smaller than today (**Figure 3**). Midge-based reconstructions in the northwest and central east and other terrestrial fauna in the northwest also registered strong early Holocene warming long before pollen-based transfer functions. This suggests no-analog vegetation communities in the early Holocene and/or long postglacial dispersal or succession lags in many parts of Greenland. One exception to the divergent response of pollen-inferred temperatures to the HTM is in the far south, where Lake Qipisarqo registered peak warmth (inferred partly from arrival of alder) for the same period of the middle Holocene as local glaciers (Fréchette & de Vernal 2009, Larocca et al. 2020a) (**Figure 3**). However, three other pollen-based records from the region indicate peak warmth after 6–5 ka, lagging evidence from local glaciers and (unlike the Qipisarqo pollen record) also showing little evidence for the late Holocene cooling recorded by glacier expansion. In other regions, by the middle Holocene pollen was overall in good agreement with other proxies, and together all indicators generally tracked subsequent long-term cooling into the late Holocene. Pollen-inferred temperatures thus appear robust at many sites through much of the middle to late Holocene, but importantly pollen does not seem to be a reliable indicator of early Holocene summer temperatures or the onset of HTM warmth in many parts of Greenland.

2.2.2. When did warmth begin? The onset of HTM warmth occurred during a time of competing climate forcings and changing boundary conditions and thus provides an opportunity to test their relative importance in driving or modulating climate change across space and time. While boreal summer insolation peaked before 9 ka (**Figure 3*e***), boreal winter insolation was at a minimum. Atmospheric carbon dioxide and total greenhouse gas forcing increased through the middle and late Holocene (**Figure 3*e***). The net influence of these primary forcings on Northern Hemisphere climate remains actively debated (Marcott et al. 2013, Marsicek et al. 2018). Furthermore, the widespread collapse of Northern Hemisphere ice sheets (**Figure 3*e***) released abundant cold, fresh meltwater to the northwest North Atlantic in the early Holocene (Jennings et al. 2015). The changing Laurentide, Innuitian, and Greenland Ice Sheets also altered local albedo and regional atmospheric circulation. The Greenland Ice Sheet had retreated to its modern margins in many regions by 10 to 9 ka or earlier, although along the central west coast it remained more extensive than today well into the middle Holocene (e.g., Carlson et al. 2014, Larsen et al. 2015, Levy et al. 2018, Sinclair et al. 2016, Søndergaard et al. 2020, Young & Briner 2015). As the ice sheets retreated, the interplay of local isostatic adjustments and eustatic sea level rise also altered the continentality of climate at some terrestrial sites and modified ocean circulation through the Arctic channels. It has long been inferred from data and models that residual, decaying ice sheets delayed postglacial warming across the northwest North Atlantic region despite enhanced summer insolation in the early Holocene (Kaufman 2004, Renssen et al. 2009)—a finding with implications for predicting how a shrinking Greenland Ice Sheet may affect future North Atlantic climate.

To pinpoint when Holocene temperatures first rose above those of the mid-twentieth century, we combine quantitative summer air temperature reconstructions with evidence from modern-day mountain glaciers and ice caps that disappeared or shrank smaller than they are today, and flora and fauna that migrated north of their current ranges for part of the Holocene. These indicators place minimum limiting ages on the onset of warmer summer temperatures because it takes time for species and ice caps to reach equilibrium with climate following a temperature shift; furthermore, taphonomy dictates that the absence of evidence for a rarely preserved thermophilous taxon is not necessarily evidence of its absence at a given location and time. We do not use past Greenland Ice Sheet extent for this purpose because of complex ice sheet dynamics and potentially long lags to reach equilibrium with climate. Nor do we use pollen-based reconstructions to identify the onset of warmth because we conclude (in Section 2.2.1) that vegetation was likely slow to reach equilibrium after deglaciation and/or reflected no-analog conditions at many Greenland sites in the early Holocene.

Overall, diverse evidence records air temperatures warmer than those of the mid-twentieth century around most of Greenland in the early Holocene (**Figures 1*b*, 2**, and **3**). The Agassiz Ice Cap experienced intense summer melt throughout the first three millennia of the Holocene (Fisher et al. 2012), when precipitation $\delta^{18}O$ at Agassiz also suggests peak annual temperatures (Lecavalier et al. 2017) (**Figure 3*a***). Midges in two lakes in adjacent northwest Greenland likewise record peak summer temperatures in the early Holocene, and the local North Ice Cap was smaller than today (Axford et al. 2019, McFarlin et al. 2018) (**Figure 3*a***). In the east, precipitation isotopes at Renland Ice Cap, chironomid assemblages, and reconstructions of smaller ice cap extent indicate temperatures exceeding those of the mid-twentieth century by ~10 ka (Axford et al. 2017, Levy et al. 2014, Lowell et al. 2013, Vinther et al. 2009) (**Figure 3*b***). Annually integrated $\delta^{18}O$, $\delta^{15}N$, and $\delta^{40}Ar$ records from Summit and NorthGRIP indicate warmer temperatures over the central ice sheet just after 10 ka (**Figure 2 *b*,*c***). Potentially consistent with all of this proxy evidence, the TraCE-$\delta^{15}N$ seasonal reconstructions suggest that summer temperatures across Greenland were warmer than those of the mid-twentieth century immediately after the Younger Dryas termination, with compensatingly low cold-season temperatures depressing annual proxy values throughout the early Holocene and especially prior to 10 ka (Buizert et al. 2018). The ice core isotope data assimilation by Badgeley et al. (2020) shows Summit temperatures reaching modern levels at ~9 ka, but this is an annual average record that has not been elevation corrected; thus, an earlier emergence of warmer-than-present summer temperatures is likely at Summit. At least some presently extant ice caps and mountain glaciers were gone or smaller than today by 9 ka in nearly all studied regions of Greenland (**Figure 3**). Terrestrial thermophiles support these continuous lines of evidence: Fredskild (1985) found an extralimital beetle species in northwest Greenland at 8.8 ka, and Funder (1978) inferred from pollen the temporary incursion of dense birch shrub tundra into the currently harsh coastal climate zone of Scoresby Sund beginning ~8.8 ka. Based upon other thermophilous plant species, Funder (1978, p. 56) also inferred that "summer temperatures were similar to the present already" before 11 ka around Scoresby Sund. Because glacier extents and species migrations lag temperature shifts, these indicators provide minimum constraints on the onset of summer temperatures warmer than those of the twentieth century.

The available data tentatively support that strong summer warming did not occur in the early Holocene in a limited area of south and possibly southwest Greenland (**Figures 1*b*** and **3*d***). All studied mountain glaciers in the south and a subset of those studied in the southwest maintained at least their present-day size until 8–7 ka (Larocca et al. 2020a,b; Larsen et al. 2017; Schweinsberg et al. 2018). Additional paleotemperature proxies are needed from the region, however, to confirm the underlying climate drivers of that glacier behavior. Depressed early Holocene warming in this small region would support climate model experiments that indicate the adjacent Labrador Sea may be especially sensitive to freshwater forcing from a shrinking Greenland Ice Sheet in the future, with widespread ramifications for overall North Atlantic climate (Liu et al. 2017, Stammer 2008). Unfortunately, the climate effects of ice sheet meltwater are understudied in future scenarios, including in the Intergovernmental Panel on Climate Change assessment reports (Bronselaer et al. 2018). Early Holocene climate provides a key opportunity to examine meltwater effects under interglacial conditions. However, models need high spatial resolution to realistically resolve the redistribution of freshwater (Condron & Winsor 2012), and data-model comparisons require accurate representations of discharge locations (Liu et al. 2017).

2.2.3. How warm were Holocene Thermal Maximum summers? Pollen records in southernmost Greenland disagree regarding the magnitude of Holocene temperature changes there

(**Figure 3*d***). This disagreement could reflect a relatively small magnitude of temperature change, which did not drive strong, regionally consistent changes in vegetation like those commonly seen further north. Larocca et al. (2020a) estimated that temperatures 1.2–1.8°C warmer than today would be adequate to cause observed middle Holocene reductions in small mountain glaciers in southernmost Greenland. Such a relatively small magnitude of summer warming in southernmost Greenland would also be consistent with the independent findings by Buizert et al. (2018) informed by climate models.

Other regions where multiproxy data are available experienced at least 3°C long-term summer temperature change through the Holocene. Around Scoresby Sund in central east Greenland, midges and pollen record 4°C or more summer cooling from the early Holocene to the preindustrial last millennium, and HTM summers approximately 3°C warmer than the mid-twentieth century (**Figure 3*b***). Early Holocene temperature anomalies recorded by midges, ice cap melt, and stable isotopes of precipitation in northwest Greenland and adjacent Ellesmere Island were even larger (Axford et al. 2019, Lecavalier et al. 2017, McFarlin et al. 2018) (**Figure 3*a***). As discussed in Sections 2.1.1 and 2.1.2, when ice core proxies from Summit are adjusted to account for changes in seasonality and ice sheet surface elevation, they suggest that HTM summers over the central ice sheet were 3.5–4.75°C warmer than in the mid-twentieth century (**Figure 2*b***).

In the central west around Disko Bugt, glaciers registered summer temperatures warmer than the mid-twentieth century in the early Holocene, but there are no local quantitative summer air temperature reconstructions for this period. Midges record ~3°C cooling there between 6 and 0.5 ka (**Figure 3*c***). Periodic reappearance of local glaciers during the early and middle Holocene may indicate this region did not warm as intensely as areas to the north and east. Near Nuuk in the southwest, Larocca et al. (2020b) estimated ~2.7°C summer cooling from the middle to late Holocene based upon reconstructed changes in glacier equilibrium line altitudes. In combination with muted warming in the south, the relatively sparse evidence from the west/southwest hints at a possible gradient in intensity of summer warming from northwest/east to south/southwest.

3. HOLOCENE THERMAL MAXIMUM SEA-SURFACE CONDITIONS SURROUNDING GREENLAND

3.1. Greenland-Region Oceanography in Relation with Climate

On a broad scale, ocean conditions around Greenland depend upon ocean heat content and the overall circulation pattern in the North Atlantic. The North Atlantic Current (NAC) carries warm, saline water to high latitudes in the subpolar basins adjacent to Greenland, including the Greenland Sea, Irminger Sea, Labrador Sea, and Baffin Bay (**Figure 1*c***). On the regional scale, neritic zone water mass properties are controlled by freshwater fluxes and meltwater discharges from the Arctic Ocean and the land mass of Greenland that are carried around the Greenland margins by currents flowing clockwise due to Coriolis forces. The East Greenland Current (EGC), fed by Arctic waters and characterized by dense sea-ice cover, carries cold, low-salinity waters southward along the eastern Greenland coast. The West Greenland Current (WGC) forms at the southern tip of Greenland from a mix of fresh, cold EGC waters and warm, saline North Atlantic waters entrained by the Irminger Current and flows northward along Greenland's west coast. Water masses around Greenland are therefore characterized by large salinity and temperature gradients from coastline to open ocean (**Figure 1*d***), depending upon the relative contribution of Arctic and Atlantic waters (**Figure 1*c***).

Salinity controls upper water mass stratification and thus plays an important role in warming of the surface layer in summer. In general, seasonal temperature contrasts are large in highly stratified surface waters of mid-high latitudes, in which low thermal inertia fosters heat uptake when solar insolation increases in summer, followed by heat release to the atmosphere in winter and cooling or freezing of surface waters. However, along continental margins upwelling generated by winds, ocean currents and/or meltwater discharge from glaciers may vertically homogenize the water column, thus breaking the stratification with consequences for primary productivity and sea-surface conditions. Hence, the wind-driven North Water and Northeast Water Polynyas, respectively located in northern Baffin Bay and off northeast Greenland, are zones marked by vertical mixing, high nutrient inputs, and cold but sea ice–free conditions most of the year (Melling et al. 2010, Morales Maqueda 2004). The glaciated margins, where outlet glaciers terminate in Greenland fjords, are also characterized by upwelling and high productivity during the late summer when meltwater discharge is maximum (Meire et al. 2017).

In summary, the regional hydrography around Greenland reflects the influences of regional meltwater and freshwater discharge in addition to heat uptake from incoming solar radiation and broad-scale ocean circulation patterns. For this reason, we separate our discussion of paleoceanographic records of offshore sites in the northern North Atlantic from those of more nearshore locations along the Greenland shelf. We summarize broad multimillennial Holocene trends in SSTs and the closely linked parameters of surface salinity and sea ice.

3.2. Offshore Records of the Holocene Thermal Maximum

On the broadest scale, the global temperature stack from Marcott et al. (2013) finds maximum temperatures from ~10 to 5 ka, and notably much of the reconstructed cooling comes from records in the North Atlantic that showed an overall ~2°C cooling from 7 ka to the nineteenth century AD. Offshore in the northwestern North Atlantic specifically, Holocene SSTs have been reconstructed using microfossil assemblages such as dinocysts (e.g., de Vernal & Hillaire-Marcel 2006, de Vernal et al. 2013, Fréchette & de Vernal 2009), planktic foraminifers (e.g., Andersson et al. 2010, Risebrobakken et al. 2003), and diatoms (e.g., Berner et al. 2011), as well as alkenones (e.g., Calvo et al. 2002, Marchal et al. 2002) and Mg/Ca in foraminifers (e.g., Came et al. 2007). From the early to late Holocene, many of these records show a general trend of gradual cooling. Particularly large amplitude SST decrease from early to late Holocene is recorded in the western sector of the North Atlantic along the route of the Gulf Stream and NAC. For example, long-term cooling close to 7°C was inferred from alkenones south of the Nova Scotia Shelf (Sachs 2007) and from dinocysts in the central northwest North Atlantic (de Vernal & Hillaire-Marcel 2006). Along the northern branches of the NAC the cooling was of lesser amplitude, in the range of 1 to 3°C south of Iceland (Marchal et al. 2002) and in eastern Fram Strait (Falardeau et al. 2018). Higher-frequency variations and site-to-site differences are described in the regional compilations of Sejrup et al. (2016) and de Vernal & Hillaire-Marcel (2006).

3.3. The Holocene Thermal Maximum off Eastern and Western Greenland

The hydrographical conditions around Greenland, including sea-ice cover and/or low surface salinity, make reconstructing sea-surface conditions challenging, notably for the alkenone and planktic foraminifer proxies commonly used for SST inferences in the open ocean. In sea-ice environments, coccolithophorid productivity is very low and the alkenone signal cannot be straightforwardly interpreted in terms of SST (Bendle et al. 2005, Moros et al. 2016, Rosell-Melé & McClymont 2007). In stratified water, with low salinity at the surface, planktic foraminifers may occupy subsurface layers below the pycnocline; this is notably the case of *Neogloboquadrina pachyderma*, the dominant taxon in polar waters (Kucera 2007). Hence, the Mg/Ca signal of their calcite shells may capture subsurface temperature instead of SST. Similarly, in a subpolar context, the use of planktic foraminifer assemblages for SST estimates is debated, as they may provide more reliable estimates of temperatures at 100 or 200 m of water depth (Telford et al. 2013), therefore documenting subsurface North Atlantic subpolar waters (McCartney & Talley 1982). In the subarctic northern North Atlantic, commonly used proxies for the reconstruction of sea-surface conditions are mostly biogenic remains from primary producers confined to the mixed layer or photic zone. They include dinocyst (e.g., de Vernal et al. 2013) and diatom assemblages (e.g., Krawczyk et al. 2010, Sha et al. 2011) in addition to biomarkers, notably IP_{25} (ice proxy with 25 carbon atoms) from ice-dwelling diatoms that allow assessment of sea-ice cover (e.g., Belt & Müller 2013, Müller et al. 2009). Benthic foraminifers from shelf areas and planktic foraminifers can also be useful, as they may carry the signal of Atlantic waters underlying the surface water layer.

Along eastern Greenland, where the cold EGC results in dense sea ice, marine records of past ocean conditions are rare except in the Denmark Strait (**Figure 1*c***). Existing records are principally based on assemblages of dinocysts (Solignac et al. 2006, Van Nieuwenhove et al. 2016), planktic and benthic foraminifers (Bauch et al. 2001, Jennings et al. 2011, Perner et al. 2016), and IP_{25} biomarkers (Müller et al. 2012, Syring et al. 2020). In the early Holocene until ∼8 ka, intense ice rafting activity and somewhat reduced production of sea-ice dwelling diatoms characterized the northern Greenland Shelf (Syring et al. 2020), while very low surface salinity, dense sea-ice cover (Solignac et al. 2006), and chilled benthic waters (cf. Perner et al. 2016) marked the Greenland shelf in the Denmark Strait (**Figure 4**), likely as a response to high meltwater discharge from rapidly waning ice on land. In the Denmark Strait area, records show variable conditions but suggest increasing salinity together with slight summer cooling and winter warming, and thus declining seasonal contrasts in temperature, from ∼8 to 4.5 ka (Solignac et al. 2006) (core JM1207, **Figure 4**). During that interval, the warm Atlantic component was relatively high in the benthic and subsurface fauna (Jennings et al. 2011, Perner et al. 2016) (cores MD99–2322 and JM1206, **Figure 4**). After 4.5 ka, higher surface salinity suggests limited glacier meltwater influx, polar fauna returned, and summer SSTs were generally cool (Jennings et al. 2002, 2011; Perner et al. 2015, 2016; Solignac et al. 2006) (**Figure 4**), while glaciers readvanced in southern Greenland fjords (Nørgaard-Pedersen & Mikkelsen 2009).

Western Greenland is bathed by the relatively warm WGC and experiences less severe sea-ice conditions than eastern Greenland. Hence, several Holocene records have been obtained, notably from the southwest Greenland fjords, Disko Bugt, Vaigat Strait, and Melville Bugt. Records of marine conditions (see examples in **Figure 5**) are mostly based on diatoms (Jensen et al. 2004; Krawczyk et al. 2010; Moros et al. 2006; Ren et al. 2009; Sha et al. 2011, 2014, 2017), foraminifers (Andresen et al. 2010; Hansen et al. 2020; Lloyd et al. 2005, 2007; Perner et al. 2012, 2013; Seidenkrantz 2007, 2013), and dinocysts (Allan et al. 2018, Caron et al. 2019, Ouellet-Bernier et al. 2014, Seidenkrantz et al. 2008). In Baffin Bay, north of Davis Strait, proxies indicate warming in the middle Holocene, with extremely harsh conditions at the surface and near-perennial sea ice until 8–7.5 ka and full interglacial conditions beginning 6 ka (Caron et al. 2019, Hansen et al. 2020, Ouellet-Bernier et al. 2014, Saini et al. 2020) (upper panels in **Figure 5**), contemporaneous with the opening of Vaigat Strait as glacier ice retreated (Lloyd et al. 2007, Perner et al. 2013). The interval after 6 ka is characterized by relatively warm proxy indicators in many of these records, but the identification of a single clear warmest period is not easy, as the proxies record complex shifts in water mass properties and show successive cooling and warming phases, all with associated chronological uncertainties. In northernmost Baffin Bay, where upwelling results in vertical mixing and opening of the North Water Polynya, the warmest surface conditions occurred ∼8 to 3 ka (Knudsen et al. 2008, Levac et al. 2001).

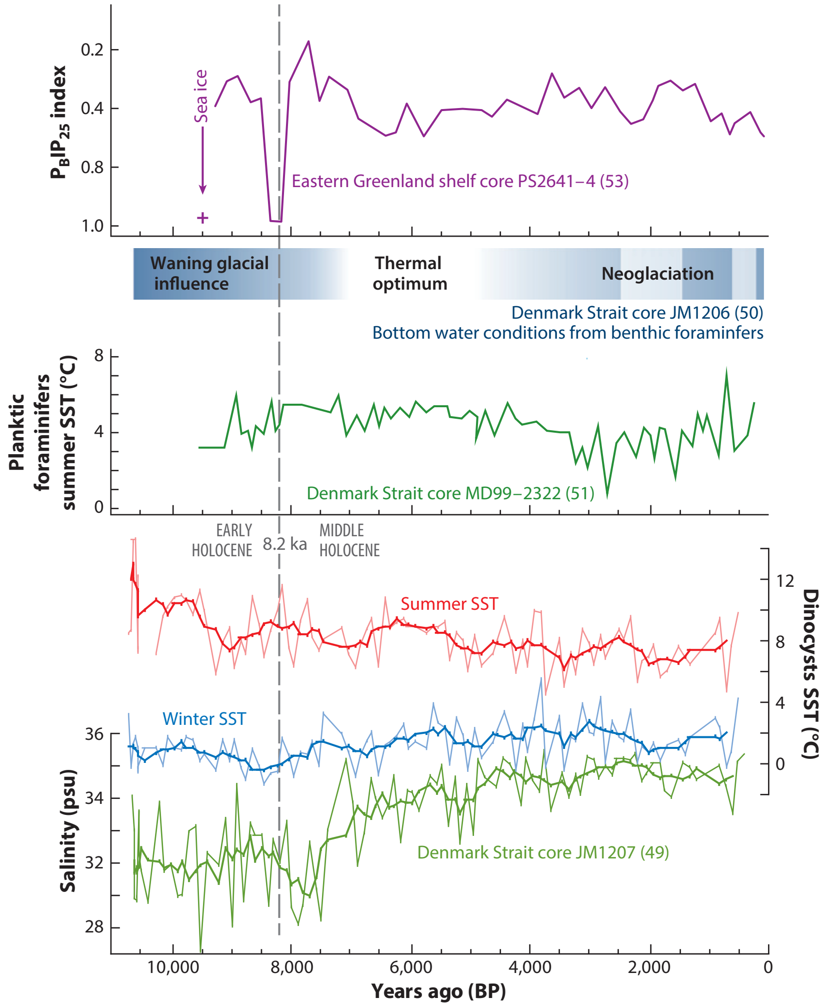

Figure 4

East Greenland marine records. From bottom: Denmark Strait salinity, summer and winter sea-surface temperature (SST) from dinocyst assemblages (Solignac et al. 2006); Denmark Strait summer SST from planktic foraminifer assemblages (Jennings et al. 2011); Denmark Strait bottom water conditions based on benthic foraminifer assemblages (Perner et al. 2016); sea-ice biomarker reconstruction from the eastern Greenland shelf (Müller et al. 2012). See **Figure 1*c*** and **Supplemental Table 1** for site information. The numbers in parentheses refer to the code numbers in **Supplemental Table 1**.

Supplemental Material >

Overall, these paleoceanographic records reveal differences between the shelf records and the overall trends from offshore sites. These differences may reflect more localized conditions on the shelf than in the open ocean, where water masses are better homogenized. The sea-surface reconstructions from the northern Labrador Sea off west Greenland (Gibb et al. 2015) (lower panel in **Figure 5**, core CC04) and the northern Irminger Basin off east Greenland (Solignac et al. 2006) (core JM1207, lower panel in **Figure 4**) may provide clues about the main trends of critical climate parameters. In both cases, the early Holocene is characterized by low salinity stabilizing in the middle Holocene after 7 ka, pointing to freshwater discharge likely related to ice sheet retreat. The SST variations of the two records are also comparable in their trends, with decreasing

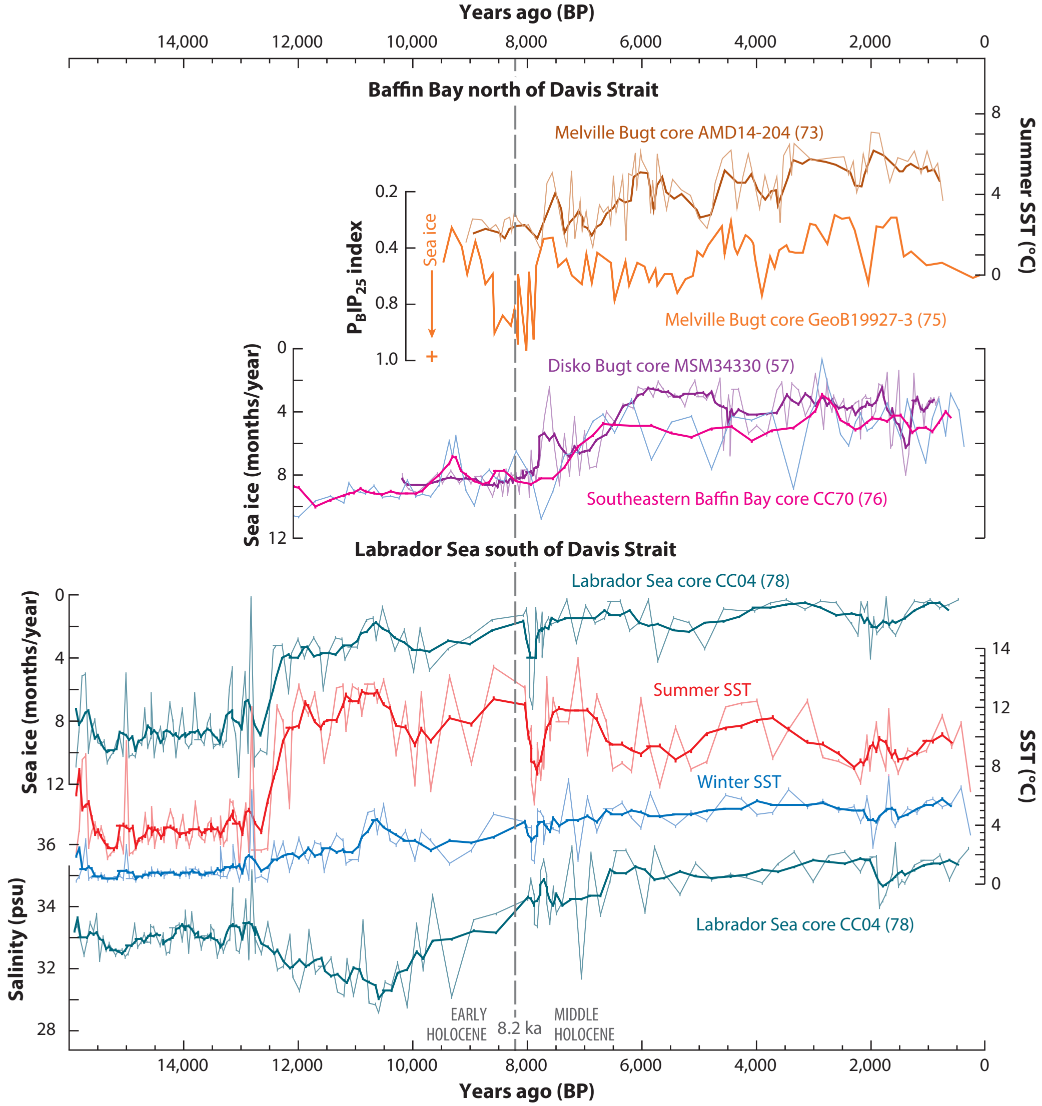

Figure 5

West Greenland marine records. South of Davis Strait, salinity, summer and winter sea-surface temperature (SST), and sea-ice cover based on dinocyst assemblages (Gibb et al. 2015). North of Davis Strait, sea-ice cover from dinocysts (Gibb et al. 2015, Ouellet-Bernier et al. 2014) and biomarkers (Saini et al. 2020) and dinocyst-based summer SST (Caron et al. 2019). See **Figure 1*c*** and **Supplemental Table 1** for site information. The numbers in parentheses refer to the code numbers in **Supplemental Table 1**.

summer temperature and slight increase of winter temperature. Hence, the summer SST data, which generally show the warmest conditions in the early Holocene until about 6 ka, are compatible with records in the path of the NAC (de Vernal & Hillaire-Marcel 2006, Falardeau et al. 2018, Marchal et al. 2002, Sachs 2007). The winter SST data are not necessarily in disagreement, but they indicate larger seasonal contrast of temperatures in the early Holocene, which is consistent with high-latitude seasonal insolation changes as well as with low salinity fostering less thermal inertia from winter to summer in the surface water layer. In contrast, cores collected on the shelf

Supplemental Material >

north of Davis Strait in Baffin Bay indicate later peak SSTs, after 6 ka and in some cases even after 3 ka, which illustrates disconnection with the more open ocean conditions of the Labrador Sea. The absence of warm conditions during the HTM along the northwest Greenland shelf likely relates to meltwater discharge from the Greenland Ice Sheet preventing northward flow of the WGC carrying Atlantic waters at the surface.

The few examples of marine records presented above illustrate a complex response under climate warming in a zone characterized by an unstable cryosphere. Locally in polar regions, meltwater discharge may result in cold and fresh surface waters unless upwelling disrupts the stratification. Distally, the mixed layer characterized by low salinity due to meltwater discharge may on the contrary experience strong summer heat uptake with insolation. The interplay of surface and subsurface currents with the salinity and density gradients in the water column strongly influences sea-surface conditions. Therefore, in a global warming perspective, the fate of the Greenland Ice Sheet is very important oceanographically, as it will interact with surface ocean properties. Ice-ocean-atmosphere dynamics around Greenland through the shifting climate of the Holocene therefore deserve further attention.

4. RECONCILING RECORDS FROM ICE, LAND, AND SEA

Two contrasting views of the Holocene in Greenland have emerged in the literature: a view of the Holocene as a relatively stable period of climate with a muted HTM centered on the middle Holocene, supported by the central Greenland ice cores, pollen, and some nearshore marine records; and an alternate view with a stronger, earlier HTM and a subsequent dramatic long-term cooling trend tracking summer insolation based primarily on ice cap retreat, nonpollen paleoecological evidence from lakes, and offshore marine records exhibiting strong long-term declines in Holocene SSTs. We find that the latter better describes regional summer air and open ocean temperature trends (**Figure 6**). The notion of middle Holocene peak warmth has arisen from a combination of terrestrial proxy issues—including varying proxy seasonality (winter temperature trends may oppose or mute summer signals in annual proxies), changes in ice sheet elevation, and vegetation lags and/or no-analog vegetation in the early Holocene—and the effects of ice sheet meltwater on sea-surface conditions. Nonpollen summer proxies from Greenland lakes show warmer and generally earlier peak Holocene temperatures than the annually integrated (and not elevation-corrected) borehole, $\delta^{18}O$, $\delta^{15}N$, and $\delta^{40}Ar$ records from the ice sheet. However, as we show in Section 2.1.2, accounting for higher ice sheet elevation in the early Holocene reconciles the apparent difference in timing, revealing peak annually integrated temperatures over the central ice sheet in the early Holocene. In contrast with most of Greenland, peak summer warmth over the south may have occurred in the middle Holocene, but evidence is limited and further research is needed to confirm that spatial variability.

The overall pattern of the HTM over Greenland—the decline in temperatures since the early Holocene registered by ice cores, glacier extents, and midges; the larger signal in summer proxies; and possibly a pattern of strongest HTM warming at the highest latitudes (**Figure 6**)—confirms the primacy of boreal summer insolation in driving Greenland summer temperatures through the Holocene. Over land, other major climate drivers including greenhouse gas concentrations, waning ice sheets, and the strength of Atlantic meridional overturning circulation had smaller or localized influences and/or primarily affected wintertime Greenland climate (Buizert et al. 2018). At sea, ice sheet meltwater had strong effects at nearshore marine sites, delaying peak SSTs especially in Baffin Bay along northwest Greenland's coast until the middle Holocene. In contrast, offshore northwest North Atlantic surface waters, particularly in the path of the NAC,

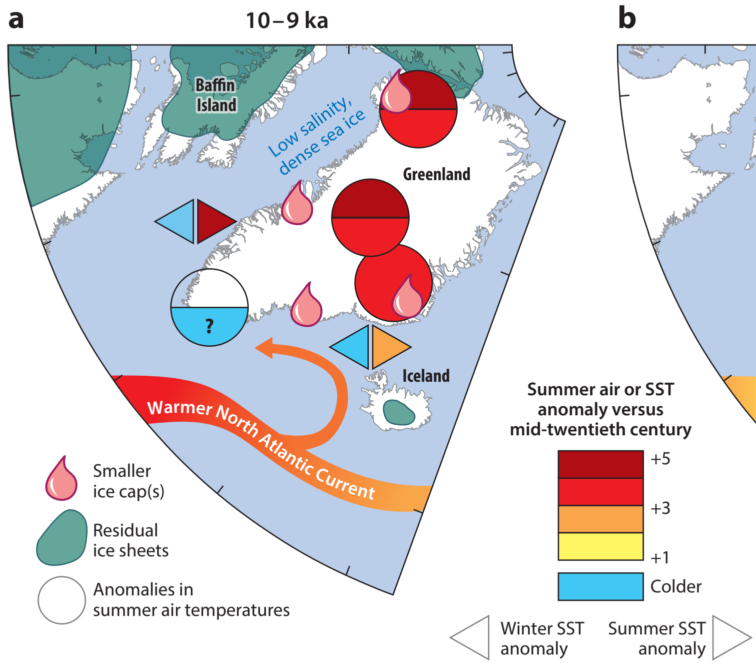

Figure 6

Summary of major climatic differences around Greenland from (*a*) 10–9 ka versus modern and (*b*) 6–5 ka versus modern, including anomalies in summer air temperature (*circles*) (estimates for Summit reflect our elevation correction of reconstructions from Buizert et al. 2018), dinocyst-inferred winter sea-surface temperature (SST) (*left triangles*) and dinocyst-inferred summer SST (*right triangles*) compared to the mid-twentieth century AD; large differences in sea-surface salinity and sea ice (*blue text*); regions with ice caps and mountain glaciers smaller than today (*pink droplets*); and major residual Pleistocene ice sheets that are now absent or very small (*green shading*). From 10 to 9 ka the Greenland Ice Sheet was thicker at Summit than today (Vinther et al. 2009) but similar in area; from 6 to 5 ka the ice sheet was smaller than today, with its minimum size poorly constrained (Larsen et al. 2015, Young & Briner 2015). Half circles reflect larger uncertainties or ranges between air temperature proxies. Unfilled triangles and half-circles indicate temperatures similar to the mid-twentieth century. Note enhanced SST seasonality in the early Holocene, with lower winter and higher summer SSTs.

experienced strong warming in the early Holocene (**Figure 6**) and generally tracked summer insolation on multimillennial timescales throughout the Holocene.

5. IMPACTS OF HOLOCENE THERMAL MAXIMUM WARMTH AND IMPLICATIONS FOR THE FUTURE

We conclude that much of Greenland experienced summer temperatures at least 3°C warmer than the mid-twentieth century in the early Holocene in response to higher boreal summer insolation (**Figure 6**). The causes of modern-day warming are unique, and there is evidence that warming in recent decades, at least at the highest latitudes, happened faster than any prior warming in the Holocene (Lecavalier et al. 2017). Nonetheless, the dramatic impacts of HTM warming hold lessons for Greenland's future. At sea, key nearshore shellfish species migrated far northward during the HTM (Bennike & Wagner 2012, Dyke et al. 1996a). The southern limit of permanent sea ice receded as much as 1,000 km inboard of its present-day limit, and bowhead whale ranges off Greenland and Canada shifted in response to complex sea-ice changes in Baffin Bay and the Arctic channels (Dyke et al. 1996b, Funder et al. 2011). On land, plant species, fish, insects, and other invertebrates migrated northward (Briner et al. 2016). HTM expansions of shrub birch, willow, and possibly alder support the expectation that shrubs will encroach on herbaceous tundra under future warming, albeit as a complex function of many factors including hydroclimate (Myers-Smith et al. 2020). Collectively, the widespread and varied responses of species to HTM climate support the prediction of trophic mismatches and other complex changes in ecological dynamics as Greenland warms rapidly in coming decades (Kerby & Post 2013).

HTM hydroclimate in Greenland is very sparsely documented but available work suggests that reduced sea ice and a warmer atmosphere led to increased winter precipitation, while warmer summers intensified evaporation and led to reduced effective moisture in the driest and warmest regions and seasons (e.g., Aebly & Fritz 2009, Anderson & Leng 2004, Meese et al. 1994, Thomas et al. 2016). Thus far, little is known about early-to-middle Holocene permafrost conditions or past wildfire status in Greenland, providing little long-term context for recent tundra wildfires widely assumed to be unprecedented (Evangeliou et al. 2019). Hydroclimate, permafrost conditions, and possibly wildfire status helped determine the net carbon-cycle effects of HTM warming over Greenland—thus, this complex parameter also remains uncertain, despite concern about carbon cycle feedbacks to future warming (Horwath Burnham & Sletten 2010, Osburn et al. 2019).

As discussed in Section 2.2.2, many Greenland mountain glaciers and ice caps disappeared during the HTM (**Figure 6**) and then grew to their present size over thousands of years in the late Holocene as summer insolation declined. Today summer insolation continues to decline, but climate is warming and the cryosphere is contracting in response to anthropogenic greenhouse gas forcing (Meier et al. 2014, Mouginot et al. 2019). So far, where Greenland's outlying glaciers have been studied, they are still larger than during the HTM despite rapid mass losses in the twentieth and twenty-first centuries. However, geologic records from the HTM imply that any prolonged future warming will cause widespread retraction of mountain glaciers and ice caps, and that many small glaciers are likely to disappear within this century (Larocca et al. 2020a, Larsen et al. 2017).

Early Holocene warming of the atmosphere and surface ocean drove rapid retreat of many sectors of the Greenland Ice Sheet (e.g., Carlson et al. 2014, Lesnek et al. 2020, Levy et al. 2020, Sinclair et al. 2016, Søndergaard et al. 2020, Young et al. 2011b). A smaller-than-present Greenland Ice Sheet is recorded by diverse evidence including early-to-middle Holocene marine materials reworked by outlet glaciers advancing during the late Holocene into formerly ice-free fjords, subfossil plants overridden and preserved beneath cold-based ice, ice-marginal lakes that currently receive ice sheet meltwater but did not for part of the Holocene, widespread early or middle Holocene ^{10}Be ages immediately outboard of present-day ice margins, and a relative sea-level history that reflects increasing glacioisostatic loading throughout the late Holocene (Farnsworth et al. 2018, Larsen et al. 2015, Long et al. 2011, Weidick & Bennike 2007, Young & Briner 2015). Most of this evidence cannot constrain how far the ice sheet retreated inland, but estimates from sparse geologic evidence and models range from 1 to 100 km inboard of present-day margins, and the extent of retreat was probably very different between regions (Young & Briner 2015). Where ice retreated, new lakes and landscapes were revealed and open-water fjords penetrated further inland. Many parts of the ice sheet receded inboard of present-day limits in the early Holocene, but it is estimated from geologic evidence that the ice sheet reached its smallest overall Holocene extent in the middle Holocene (Larsen et al. 2015, Young & Briner 2015).

Rates of retreat during the HTM varied widely. Holocene retreat rates of 10–20 m/year are documented in several areas and up to 100 m/year for the outlet glacier Sermeq Kujalleq/Jakobshavn Isbrae (Lesnek & Briner 2018, Young et al. 2011b). On a broader scale, Larsen et al. (2015) estimated 100 Gt/year mass loss throughout several millennia from the entire ice sheet, comparable to its average estimated rate of mass loss in the past four decades. Due to recent acceleration of mass loss, rates of loss since ~2000 AD are much higher than that 40-year average

(Mouginot et al. 2019). Over the southwest quadrant of the ice sheet, observed rapid mass loss since 2000 AD rivals modeled HTM retreat rates, and further warming this century is predicted to drive faster mass loss than modeled for the HTM (Briner et al. 2020). Estimates of the ice sheet's sensitivity to HTM warmth are complicated by the ice sheet's prior history, in which it expanded to Greenland's continental shelves during the Last Glacial Maximum and its marine-based portions subsequently collapsed in response at least partly to glacial-interglacial warming at the last glacial termination. Adding to the complexity, some margins also briefly advanced during century-scale cold snaps in the early Holocene, including at 8.2 ka (Young et al. 2011a).

Overall, geologic evidence from the HTM supports that future warming will cause significant retraction of the ice sheet at variable and highly uncertain rates. It is also worth noting that much of the ice sheet survived several millennia of early-to-middle Holocene summers significantly warmer than those of the mid-twentieth century. Both observations provide useful constraints for testing the performance of ice sheet models. But note the importance to that exercise of realistically characterizing Holocene seasonality: Glacier surface melt is driven by warm-season temperatures around the ice sheet's margins, and thus ice sheet models driven by paleotemperature reconstructions from annual proxies may produce erroneously small and slow mass balance changes during the HTM (e.g., Simpson et al. 2009).

Meltwater from the shrinking Greenland Ice Sheet had profound effects on nearshore marine environments and sea-surface conditions around Greenland during the HTM. Evidence for delayed HTM warming in southern Greenland, alongside model simulations of meltwater effects on convection in the Labrador Sea, suggests that acceleration of meltwater discharge from future ice sheet retreat could fundamentally alter sea-surface conditions in Baffin Bay and the Labrador Sea. This in turn may affect convection in the Labrador Sea and potentially the Atlantic meridional overturning circulation and global climate (Rahmstorf et al. 2015).

The fate of the Greenland Ice Sheet is globally important due to its role in sea level, ocean circulation, and climatic conditions throughout the circum-Atlantic region. As reviewed here, Holocene reconstructions from ice, lake sediments, and marine cores reveal that diverse and dramatic environmental changes including significant ice sheet retreat accompanied the last protracted period of warmer climate in Greenland. Future investigations of the HTM should further resolve how much, how quickly, and in what seasons climate there responds to external forcings, and how the complex interactions between Greenland's ice, ocean, and atmosphere unfold in a warming climate.

SUMMARY POINTS

1. The pattern of Holocene Thermal Maximum (HTM) warmth around Greenland confirms the primacy of boreal summer insolation in driving Holocene air temperatures there prior to anthropogenic warming. Summer air temperatures rose above those of the mid-twentieth century AD in the early Holocene around much of Greenland, and indeed by 10 ka in many regions including over the central ice sheet. Open ocean temperatures also peaked in the early Holocene. In the south and southwest, summer air temperatures may have remained comparable to or below those of the mid-twentieth century until the middle Holocene.
2. Maximum Holocene summer air temperature anomalies probably varied spatially across Greenland, from 3 to 5°C warmer than the mid-twentieth century in the northwest and over the central ice sheet to 1 to 2°C in the south. Although it has some support from

climate models, this observed spatial pattern is based on a small number of summer temperature records. Additional paleolimnological records and summer reconstructions from ice cores are needed. The spatial pattern of Holocene temperature shifts will provide a target for model simulations examining how diverse forcings and feedbacks affect climate in the high-latitude North Atlantic region.

3. Apparent differences between ice cores and lake sediment records can be resolved with attention to seasonality and to ice sheet surface elevation changes, which when ignored both tend to mask summer warming over the ice sheet in the early Holocene. Summer temperatures must be accurately resolved to provide meaningful assessments of past ice sheet responses to climate change because summer temperatures drive ice surface mass loss.
4. Pollen-inferred temperatures diverge from other indicators in the early Holocene, suggesting vegetation migration lags and/or no-analog climates that should be investigated in future research. However, pollen-inferred temperature trends at most sites agree well with other proxies through the middle and late Holocene.
5. North Atlantic waters carried with the North Atlantic Current brought very warm conditions offshore of southern Greenland in the early Holocene. At the same time, freshwater discharge resulting from rapid waning of the Greenland Ice Sheet led to strong stratification of surface waters, increased winter sea ice, cold winters, and warm summers closer to Greenland's coasts. Given the likelihood of enhanced freshwater discharge from the Greenland Ice Sheet in the future, paleoclimatologists should prioritize understanding these early Holocene dynamics.
6. Well-documented impacts of HTM warming around Greenland included loss of many glaciers and ice caps; retreat of the Greenland Ice Sheet; lower sea-surface salinity due to high meltwater discharge, resulting in dense winter sea ice despite high summer sea-surface temperatures offshore and thus large seasonal contrasts of temperatures; and widespread migrations of marine and terrestrial flora and fauna. Effects on hydroclimate and carbon cycling are only sparsely documented and should be targets for future research.

DISCLOSURE STATEMENT

The authors are not aware of any affiliations, memberships, funding, or financial holdings that might be perceived as affecting the objectivity of this review.

ACKNOWLEDGMENTS

First and foremost, we thank the people of Kalaallit Nunaat (known in English as Greenland) for welcoming scientists from around the world who grow fascinated by their homeland. Research by countless colleagues has catalyzed understanding of Greenland's Holocene climate, including many studies that regrettably could not be cited due to space limitations. Christo Buizert, Konrad Gajewski, Anne Jennings, Chris Kuzawa, Laura Larocca, Nicolaj Larsen, Peter Puleo, Regan Steigleder, and John (Jack) Williams provided helpful comments and discussion. This review was supported by US National Science Foundation CAREER grant OPP-1454734, the Natural Sciences and Engineering Research Council of Canada, and the Fonds de Recherche du Québec–Nature et Technologies.

LITERATURE CITED

Aebly FA, Fritz SC. 2009. Palaeohydrology of Kangerlussuaq (Søndre Strømfjord), West Greenland during the last ~8000 years. *Holocene* 19:91–104

Allan E, de Vernal A, Knudsen MF, Hillaire-Marcel C, Moros M, et al. 2018. Late Holocene sea surface instabilities in the Disko Bugt area, West Greenland, in phase with $\delta^{18}O$ oscillations at Camp Century. *Paleoceanogr. Paleoclimatol.* 33:227–43

Alley RB, Anandakrishnan S. 1995. Variations in melt-layer frequency in the GISP2 ice core: implications for Holocene summer temperatures in central Greenland. *Ann. Glaciol.* 21:64–70

Anderson NJ, Leng MJ. 2004. Increased aridity during the early Holocene in West Greenland inferred from stable isotopes in laminated-lake sediments. *Quat. Sci. Rev.* 23:841–49

Andersson C, Pausata FSR, Jansen E, Risebrobakken B, Telford RJ. 2010. Holocene trends in the foraminifer record from the Norwegian Sea and the North Atlantic Ocean. *Clim. Past* 6:179–93

Andresen CS, McCarthy DJ, Valdemar Dylmer C, Seidenkrantz M-S, Kuijpers A, Lloyd JM. 2010. Interaction between subsurface ocean waters and calving of the Jakobshavn Isbræ during the late Holocene. *Holocene* 21:211–24

Axford Y, Lasher GE, Kelly MA, Osterberg EC, Landis J, et al. 2019. Holocene temperature history of northwest Greenland—with new ice cap constraints and chironomid assemblages from Deltasø. *Quat. Sci. Rev.* 215:160–72

Axford Y, Levy LB, Kelly MA, Francis DR, Hall BL, et al. 2017. Timing and magnitude of early to middle Holocene warming in East Greenland inferred from chironomids. *Boreas* 46(4):678–87

Axford Y, Losee S, Briner JP, Francis DR, Langdon PG, Walker IR. 2013. Holocene temperature history at the western Greenland Ice Sheet margin reconstructed from lake sediments. *Quat. Sci. Rev.* 59:87–100

Badgeley JA, Steig EJ, Hakim GJ, Fudge TJ. 2020. Greenland temperature and precipitation over the last 20000 years using data assimilation. *Clim. Past* 16:1325–46

Balascio NL, D'Andrea WJ, Bradley RS. 2015. Glacier response to North Atlantic climate variability during the Holocene. *Clim. Past* 11:1587–98

Bauch HA, Erlenkeuser H, Spielhagen R, Struck U, Matthiessen J, et al. 2001. A multiproxy reconstruction of the evolution of deep and surface waters in the subarctic Nordic seas over the last 30,000 yr. *Quat. Sci. Rev.* 20:659–78

Belt ST, Müller J. 2013. The Arctic sea ice biomarker IP_{25}: a review of current understanding, recommendations for future research and applications in palaeo sea ice reconstructions. *Quat. Sci. Rev.* 79:9–25

Bendle J, Rosell-Melé A, Ziveri P. 2005. Variability of unusual distributions of alkenones in the surface waters of the Nordic seas. *Paleoceanography* 20:PA2001

Bennike O, Anderson NJ, McGowan S. 2010. Holocene palaeoecology of southwest Greenland inferred from macrofossils in sediments of an oligosaline lake. *J. Paleolimnol.* 43:787–98

Bennike O, Wagner B. 2012. Holocene range of *Mytilus edulis* in central East Greenland. *Polar Rec*. 49:291–96

Berger A, Loutre M-F. 1991. Insolation values for the climate of the last 10 million years. *Quat. Sci. Rev.* 10:297–317

Berner KS, Koç N, Godtliebsen F, Divine D. 2011. Holocene climate variability of the Norwegian Atlantic Current during high and low solar insolation forcing. *Paleoceanography* 26:PA2220

Briner JP, Cuzzone JK, Badgeley JA, Young NE, Steig EJ, et al. 2020. Rate of mass loss from the Greenland Ice Sheet will exceed Holocene values this century. *Nature* 586:70–74

Briner JP, McKay NP, Axford Y, Bennike O, Bradley RS, et al. 2016. Holocene climate change in Arctic Canada and Greenland. *Quat. Sci. Rev.* 147:340–64

Brodersen KP, Anderson NJ. 2002. Distribution of chironomids (Diptera) in low arctic West Greenland lakes: trophic conditions, temperature and environmental reconstruction. *Freshw. Biol.* 47:1137–57

Bronselaer B, Winton M, Griffies SM, Hurlin WJ, Rodgers KB, et al. 2018. Change in future climate due to Antarctic meltwater. *Nature* 564:53–58

Buizert C, Keisling BA, Box JE, He F, Carlson AE, et al. 2018. Greenland-wide seasonal temperatures during the last deglaciation. *Geophys. Res. Lett.* 45:1905–14

Calvo E, Grimalt JO, Jansen E. 2002. High resolution U_{37}^{K} sea surface temperature reconstruction in the Norwegian Sea during the Holocene. *Quat. Sci. Rev.* 21:1385–94

Came RE, Oppo DW, McManus JF. 2007. Amplitude and timing of temperature and salinity variability in the subpolar North Atlantic over the past 10 k.y. *Geology* 35:315–18

Carlson AE, Winsor K, Ullman DJ, Brook EJ, Rood DH, et al. 2014. Earliest Holocene south Greenland ice sheet retreat within its late Holocene extent. *Geophys. Res. Lett.* 41:5514–21

Caron M, Rochon A, Montero-Serrano J-C, St-Onge G. 2019. Evolution of sea-surface conditions on the northwestern Greenland margin during the Holocene. *J. Quat. Sci.* 34:569–80

Clark PU, Shakun JD, Marcott SA, Mix AC, Eby M, et al. 2016. Consequences of twenty-first-century policy for multi-millennial climate and sea-level change. *Nat. Clim. Change* 6:360–69

Condron A, Winsor P. 2012. Meltwater routing and the Younger Dryas. *PNAS* 109:19928–33

Crump SE, Miller GH, Power M, Sepulveda J, Dildar N, et al. 2019. Arctic shrub colonization lagged peak postglacial warmth: molecular evidence in lake sediment from Arctic Canada. *Glob. Change Biol.* 25:4244–56

Cuffey KM, Clow GD. 1997. Temperature, accumulation, and ice sheet elevation in central Greenland through the last deglacial transition. *J. Geophys. Res.* 102(C12):26383–96

D'Andrea WJ, Huang Y, Fritz SC, Anderson NJ. 2011. Abrupt Holocene climate change as an important factor for human migration in West Greenland. *PNAS* 108:9765–69

Dahl-Jensen D, Mosegaard K, Gundestrup N, Clow GD, Johnsen SJ, Hansen AW, Balling N. 1998. Past temperatures directly from the Greenland Ice Sheet. *Science* 282:268–71

Dalton AS, Margold M, Stokes CR, Tarasov L, Dyke AS, et al. 2020. An updated radiocarbon-based ice margin chronology for the last deglaciation of the North American Ice Sheet Complex. *Quat. Sci. Rev.* 234:106223

Dansgaard W. 1961. *The Isotopic Composition of Natural Waters with Special Reference to the Greenland Ice Cap.* Copenhagen, Den.: C.A. Reitzel

de Vernal A, Hillaire-Marcel C. 2006. Provincialism in trends and high frequency changes in the northwest North Atlantic during the Holocene. *Glob. Planet. Change* 54:263–90

de Vernal A, Hillaire-Marcel C, Rochon A, Fréchette B, Henry M, et al. 2013. Dinocyst-based reconstructions of sea ice cover concentration during the Holocene in the Arctic Ocean, the northern North Atlantic Ocean and its adjacent seas. *Quat. Sci. Rev.* 79:111–21

Dyke AS, Dale JE, McNeely RN. 1996a. Marine molluscs as indicators of environmental change in glaciated North America and Greenland during the last 18000 years. *Géogr. Phys. Quat.* 50:125–84

Dyke AS, Hooper J, Savelle J. 1996b. A history of sea ice in the Canadian Arctic Archipelago based on postglacial remains of the bowhead whale (*Balaena mysticetus*). *Arctic* 49:235–55

Edwards ME, Brubaker LB, Lozhkin AV, Anderson PM. 2005. Structurally novel biomes: a response to past warming in Beringia. *Ecology* 86:1696–703

Evangeliou N, Kylling A, Eckhardt S, Myroniuk V, Stebel K, et al. 2019. Open fires in Greenland in summer 2017: transport, deposition and radiative effects of BC, OC and BrC emissions. *Atmos. Chem. Phys.* 19:1393–411

Falardeau J, de Vernal A, Spielhagen RF. 2018. Paleoceanography of northeastern Fram Strait since the last glacial maximum: palynological evidence of large amplitude changes. *Quat. Sci. Rev.* 195:133–52

Farnsworth LB, Kelly MA, Bromley GRM, Axford Y, Osterberg EC, et al. 2018. Holocene history of the Greenland Ice-Sheet margin in Northern Nunatarssuaq, Northwest Greenland. *Arktos* 4:1–27

Fisher D, Zheng J, Burgess D, Zdanowicz C, Kinnard C, et al. 2012. Recent melt rates of Canadian arctic ice caps are the highest in four millennia. *Glob. Planet. Change* 84–85:3–7

Fréchette B, de Vernal A. 2009. Relationship between Holocene climate variations over southern Greenland and eastern Baffin Island and synoptic circulation pattern. *Clim. Past* 5:347–59

Fréchette B, de Vernal A, Guiot J, Wolfe AP, Miller GH, et al. 2008. Methodological basis for quantitative reconstruction of air temperature and sunshine from pollen assemblages in Arctic Canada and Greenland. *Quat. Sci. Rev.* 27:1197–216

Fredskild B. 1985. The Holocene vegetational development of Tugtuligssuaq and Qeqertat, Northwest Greenland. *Medd. Grønl.* 14:1–20

Funder S. 1978. Holocene stratigraphy and vegetation history in the Scoresby Sund area, East Greenland. *Bull. Groenl. Geol. Unders.* 12:1–76

Funder S, Goosse H, Jepsen H, Kaas E, Kjær KH, et al. 2011. A 10,000-year record of Arctic Ocean sea-ice variability—view from the beach. *Science* 333:747–50

Gajewski K. 2015a. Impact of Holocene climate variability on Arctic vegetation. *Glob. Planet. Change* 133:272–87

Gajewski K. 2015b. Quantitative reconstruction of Holocene temperatures across the Canadian Arctic and Greenland. *Glob. Planet. Change* 128:14–23

Gibb OT, Steinhauer S, Fréchette B, de Vernal A, Hillaire-Marcel C. 2015. Diachronous evolution of sea surface conditions in the Labrador Sea and Baffin Bay since the last deglaciation. *Holocene* 25:1882–97

Graeter KA, Osterberg EC, Ferris DG, Hawley RL, Marshall HP, et al. 2018. Ice core records of West Greenland melt and climate forcing. *Geophys. Res. Lett.* 45:3164–72

Hansen KE, Giraudeau J, Wacker L, Pearce C, Seidenkrantz M-S. 2020. Reconstruction of Holocene oceanographic conditions in the Northeastern Baffin Bay. *Clim. Past* 16:1075–95

Horwath Burnham J, Sletten RS. 2010. Spatial distribution of soil organic carbon in northwest Greenland and underestimates of high Arctic carbon stores. *Glob. Biogeochem. Cycles* 24:GB3012

Iversen J. 1952. Origin of the flora of western Greenland in the light of pollen analysis. *Oikos* 4:85–103

Jennings A, Andrews J, Pearce C, Wilson L, Ólfasdótttir S. 2015. Detrital carbonate peaks on the Labrador shelf, a 13–7 ka template for freshwater forcing from the Hudson Strait outlet of the Laurentide Ice Sheet into the subpolar gyre. *Quat. Sci. Rev.* 107:62–80

Jennings A, Andrews J, Wilson L. 2011. Holocene environmental evolution of the SE Greenland Shelf North and South of the Denmark Strait: Irminger and East Greenland current interactions. *Quat. Sci. Rev.* 30:980–98

Jennings AE, Knudsen K, Hald M, Hansen CV, Andrews JT. 2002. A mid-Holocene shift in Arctic sea-ice variability on the East Greenland Shelf. *Holocene* 12:49–58

Jensen KG, Kuijpers A, Koç N, Heinemeier J. 2004. Diatom evidence of hydrographic changes and ice conditions in Igaliku Fjord, South Greenland, during the past 1500 years. *Holocene* 14:152–64

Johnsen SJ, Dahl-Jensen D, Dansgaard W, Gundestrup N. 1995. Greenland paleotemperatures derived from GRIP bore hole temperature and ice core isotope profiles. *Tellus B: Chem. Phys. Meteorol.* 47:624–29

Johnsen SJ, Dahl-Jensen D, Gundestrup N, Steffensen JP, Clausen HB, et al. 2001. Oxygen isotope and palaeotemperature records from six Greenland ice-core stations: Camp Century, Dye-3, GRIP, GISP2, Renland and NorthGRIP. *J. Quat. Sci.* 16:299–307

Kaufman D. 2004. Holocene thermal maximum in the western Arctic (0–180°W). *Quat. Sci. Rev.* 23:529–60

Kaufman D, McKay N, Routson C, Erb M, Davis B, et al. 2020. A global database of Holocene paleotemperature records. *Sci. Data* 7:115

Kaufman DS, Schneider DP, McKay NP, Ammann CM, Bradley RS, et al. 2009. Recent warming reverses long-term arctic cooling. *Science* 325:1236–39

Kelly MA, Lowell TV. 2009. Fluctuations of local glaciers in Greenland during latest Pleistocene and Holocene time. *Quat. Sci. Rev.* 28:2088–106

Kerby JT, Post E. 2013. Advancing plant phenology and reduced herbivore production in a terrestrial system associated with sea ice decline. *Nat. Commun.* 4:2514

Knudsen KL, Søndergaard MKB, Eiríksson J, Jiang H. 2008. Holocene thermal maximum off North Iceland: evidence from benthic and planktonic foraminifera in the 8600–5200 cal year BP time slice. *Mar. Micropaleontol.* 67:120–42

Kobashi T, Menviel L, Jeltsch-Thommes A, Vinther BM, Box JE, et al. 2017. Volcanic influence on centennial to millennial Holocene Greenland temperature change. *Sci. Rep.* 7:1441

Krawczyk D, Witkowski A, Moros M, Lloyd J, Kuijpers A, Kierzek A. 2010. Late-Holocene diatom-inferred reconstruction of temperature variations of the West Greenland Current from Disko Bugt, central West Greenland. *Holocene* 20:659–66

Kucera M. 2007. Planktonic foraminifera as tracers of past oceanic environments. In *Proxies in Late Cenozoic Paleoceanography*, ed. C Hillaire-Marcel, A de Vernal, pp. 213–62. Amsterdam: Elsevier

Larocca LJ, Axford Y, Bjørk AA, Lasher GE, Brooks JP. 2020a. Local glaciers record delayed peak Holocene warmth in south Greenland. *Quat. Sci. Rev.* 241:106421

Larocca LJ, Axford Y, Woodroffe SA, Lasher GE, Gawin B. 2020b. Holocene glacier and ice cap fluctuations in southwest Greenland inferred from two lake records. *Quat. Sci. Rev.* 246:106529

Larsen NK, Kjær KH, Lecavalier B, Bjørk AA, Colding S, et al. 2015. The response of the southern Greenland ice sheet to the Holocene thermal maximum. *Geology* 43:291–94

Larsen NK, Levy LB, Strunk A, Søndergaard AS, Olsen J, Lauridsen TL. 2019. Local ice caps in Finderup Land, North Greenland, survived the Holocene Thermal Maximum. *Boreas* 48:551–62

Larsen NK, Strunk A, Levy LB, Olsen J, Bjørk A, et al. 2017. Strong altitudinal control on the response of local glaciers to Holocene climate change in southwest Greenland. *Quat. Sci. Rev.* 168:69–78

Lasher GE, Axford Y, Masterson AL, Berman K, Larocca LJ. 2020. Holocene temperature and landscape history of southwest Greenland inferred from isotope and geochemical lake sediment proxies. *Quat. Sci. Rev.* 239:106358

Lasher GE, Axford Y, McFarlin JM, Kelly MA, Osterberg EC, Berkelhammer MB. 2017. Holocene temperatures and isotopes of precipitation in Northwest Greenland recorded in lacustrine organic materials. *Quat. Sci. Rev.* 170:45–55

Lecavalier BS, Fisher DA, Milne GA, Vinther BM, Tarasov L, et al. 2017. High Arctic Holocene temperature record from the Agassiz ice cap and Greenland ice sheet evolution. *PNAS* 114:5952–57

Lecavalier BS, Milne GA, Vinther BM, Fisher DA, Dyke AS, Simpson MJR. 2013. Revised estimates of Greenland ice sheet thinning histories based on ice-core records. *Quat. Sci. Rev.* 63:73–82

Lesnek AJ, Briner JP. 2018. Response of a land-terminating sector of the western Greenland Ice Sheet to early Holocene climate change: evidence from ^{10}Be dating in the Søndre Isortoq region. *Quat. Sci. Rev.* 180:145–56

Lesnek AJ, Briner JP, NE Young, Cuzzone JK. 2020. Maximum southwest Greenland ice sheet recession in the early Holocene. *Geophys. Res. Lett.* 47:e2019GL083164

Levac E, Vernal AD, Blake W Jr. 2001. Sea-surface conditions in northernmost Baffin Bay during the Holocene: palynological evidence. *J. Quat. Sci.* 16:353–63

Levy LB, Kelly MA, Applegate PA, Howley JA, Virginia RA. 2018. Middle to late Holocene chronology of the western margin of the Greenland Ice Sheet: a comparison with Holocene temperature and precipitation records. *Arct. Antarct. Alp. Res.* 50:S100004

Levy LB, Kelly MA, Lowell TV, Hall BL, Hempel LA, et al. 2014. Holocene fluctuations of Bregne ice cap, Scoresby Sund, east Greenland: a proxy for climate along the Greenland Ice Sheet margin. *Quat. Sci. Rev.* 92:357–68

Levy LB, Larsen NK, Knudsen MF, Egholm DL, Bjørk AA, et al. 2020. Multi-phased deglaciation of south and southeast Greenland controlled by climate and topographic setting. *Quat. Sci. Rev.* 242:106454

Liu Y, Hallberg R, Sergienko O, Samuels BL, Harrison M, Oppenheimer M. 2017. Climate response to the meltwater runoff from Greenland ice sheet: evolving sensitivity to discharging locations. *Clim. Dyn.* 51:1733–51

Liu Z, Otto-Bliesner BL, He F, Brady EC, Tomas R, et al. 2009. Transient simulation of last deglaciation with a new mechanism for Bølling-Allerød warming. *Science* 325:310–14

Lloyd JM, Kuijpers A, Long A, Moros M, Park LA. 2007. Foraminiferal reconstruction of mid- to late-Holocene ocean circulation and climate variability in Disko Bugt, West Greenland. *Holocene* 17:1079–91

Lloyd JM, Park LA, Kuijpers A, Moros M. 2005. Early Holocene palaeoceanography and deglacial chronology of Disko Bugt, West Greenland. *Quat. Sci. Rev.* 24:1741–55

Long AJ, Woodroffe SA, Roberts DH, Dawson S. 2011. Isolation basins, sea-level changes and the Holocene history of the Greenland Ice Sheet. *Quat. Sci. Rev.* 30:3748–68

Lowell TV, Hall BL, Kelly MA, Bennike O, Lusas AR, et al. 2013. Late Holocene expansion of Istorvet ice cap, Liverpool Land, east Greenland. *Quat. Sci. Rev.* 63:128–40

Marchal O, Cacho I, Stocker TF, Grimalt JO, Calvo E, et al. 2002. Apparent long-term cooling of the sea surface in the northeast Atlantic and Mediterranean during the Holocene. *Quat. Sci. Rev.* 21:455–83

Marcott SA, Shakun JD, Clark PU, Mix AC. 2013. A reconstruction of regional and global temperature for the past 11,300 years. *Science* 339:1198–201

Marsicek J, Shuman BN, Bartlein PJ, Shafer SL, Brewer S. 2018. Reconciling divergent trends and millennial variations in Holocene temperatures. *Nature* 554:92–96

Masson-Delmotte V, Landais A, Stievenard M, Cattani O, Falourd S, et al. 2005. Holocene climatic changes in Greenland: different deuterium excess signals at Greenland Ice Core Project (GRIP) and NorthGRIP. *J. Geophys. Res.* 110(D14):D14102

McCartney MS, Talley LD. 1982. The subpolar mode water of the North Atlantic Ocean. *J. Phys. Oceanogr.* 12:1169–88

McFarlin JM, Axford Y, Osburn MR, Kelly MA, Osterberg EC, Farnsworth LB. 2018. Pronounced summer warming in northwest Greenland during the Holocene and Last Interglacial. *PNAS* 155:6357–62

McGrath D, Colgan W, Bayou N, Muto A, Steffen K. 2013. Recent warming at Summit, Greenland: global context and implications. *Geophys. Res. Lett.* 40:2091–96

Meese D, Gow A, Grootes P, Ram M, Stuiver M, et al. 1994. The accumulation record from the GISP2 core as an indicator of climate change throughout the Holocene. *Science* 266:1680–82

Meire L, Mortensen J, Meire P, Juul-Pedersen T, Sejr MK, et al. 2017. Marine-terminating glaciers sustain high productivity in Greenland fjords. *Glob. Change Biol.* 23:5344–57

Meier WN, Hovelsrud GK, van Oort BEH, Key JR, Kovacs KM, et al. 2014. Arctic sea ice in transformation: a review of recent observed changes and impacts on biology and human activity. *Rev. Geophys.* 52:185–217

Melling H, Gratton Y, Ingram G. 2010. Ocean circulation within the North Water Polynya of Baffin Bay. *Atmosphere-Ocean* 39:301–25

Minor K, Agneman G, Davidsen N, Kleemann N, Markussen U, et al. 2019. *Greenlandic perspectives on climate change 2018–2019: results from a national survey*. Rep., Univ. Greenl., Univ. Cph., Kraks Fond Inst. Urban Res., Copenhagen, Den.

Monnin E, Steig EJ, Siegenthaler U, Kawamura K, Schwander J, et al. 2004. Evidence for substantial accumulation rate variability in Antarctica during the Holocene, through synchronization of CO_2 in the Taylor Dome, Dome C and DML ice cores. *Earth Planet. Sci. Lett.* 224:45–54

Morales Maqueda MA. 2004. Polynya dynamics: a review of observations and modeling. *Rev. Geophys.* 42:RG1004

Moros M, Andrews JT, Eberl DD, Jansen E. 2006. Holocene history of drift ice in the northern North Atlantic: evidence for different spatial and temporal modes. *Paleoceanography* 21:PA201

Moros M, Lloyd JM, Perner K, Krawczyk D, Blanz T, et al. 2016. Surface and sub-surface multi-proxy reconstruction of middle to late Holocene palaeoceanographic changes in Disko Bugt, West Greenland. *Quat. Sci. Rev.* 132:146–60

Mouginot J, Rignot E, Bjork AA, van den Broeke M, Millan R, et al. 2019. Forty-six years of Greenland Ice Sheet mass balance from 1972 to 2018. *PNAS* 116:9239–44

Müller J, Massé G, Stein R, Belt ST. 2009. Variability of sea-ice conditions in the Fram Strait over the past 30,000 years. *Nat. Geosci.* 2:772–76

Müller J, Werner K, Stein R, Fahl K, Moros M, Jansen E. 2012. Holocene cooling culminates in sea ice oscillations in Fram Strait. *Quat. Sci. Rev.* 47:1–14

Myers-Smith IH, Kerby JT, Phoenix GK, Bjerke JW, Epstein HE, et al. 2020. Complexity revealed in the greening of the Arctic. *Nat. Clim. Change* 10:106–17

Natl. Snow Ice Data Cent. 2020. *Data and image archive*. Sea ice index, updated daily. **https://nsidc.org/data/seaice_index/archives**

NCEI (Natl. Cent. Environ. Inf.). 2009. *Objective analyses and statistics*. World Ocean Atlas 2009, updated Apr. 25, 2015. **https://www.nodc.noaa.gov/OC5/WOA09/woa09data.html**

Nghiem SV, Hall DK, Mote TL, Tedesco M, Albert MR, et al. 2012. The extreme melt across the Greenland ice sheet in 2012. *Geophys. Res. Lett.* 39:L20502

Nørgaard-Pedersen N, Mikkelsen N. 2009. 8000 year marine record of climate variability and fjord dynamics from Southern Greenland. *Mar. Geol.* 264:177–89

Ohmura A. 1987. New temperature distribution maps for Greenland. *Z. Gletsch. Glazialgeol.* 23:1–45

Osburn CL, Anderson NJ, Leng MJ, Barry CD, Whiteford EJ. 2019. Stable isotopes reveal independent carbon pools across an Arctic hydro-climatic gradient: implications for the fate of carbon in warmer and drier conditions. *Limnol. Oceanogr. Lett.* 4:205–13

Ouellet-Bernier M-M, de Vernal A, Hillaire-Marcel C, Moros M. 2014. Paleoceanographic changes in the Disko Bugt area, West Greenland, during the Holocene. *Holocene* 24:1573–83

Perner K, Jennings AE, Moros M, Andrews JT, Wacker L. 2016. Interaction between warm Atlantic-sourced waters and the East Greenland Current in northern Denmark Strait (68°N) during the last 10600 cal a BP. *J. Quat. Sci.* 31:472–83

Perner K, Moros M, Jennings A, Lloyd JM, Knudsen KL. 2012. Holocene palaeoceanographic evolution off West Greenland. *Holocene* 23:374–87

Perner K, Moros M, Lloyd JM, Jansen E, Stein R. 2015. Mid to late Holocene strengthening of the East Greenland Current linked to warm subsurface Atlantic water. *Quat. Sci. Rev.* 129:296–307

Perner K, Moros M, Snowball I, Lloyd JM, Kuijpers A, Richter T. 2013. Establishment of modern circulation pattern at c. 6000 cal a BP in Disko Bugt, central West Greenland: opening of the Vaigat Strait. *J. Quat. Sci.* 28:480–89

Rahmstorf S, Box JE, Feulner G, Mann ME, Robinson A, et al. 2015. Exceptional twentieth-century slowdown in Atlantic Ocean overturning circulation. *Nat. Clim. Change* 5:475–80

Rasmussen SO, Andersen KK, Svensson AM, Steffensen JP, Vinther BM, et al. 2006. A new Greenland ice core chronology for the last glacial termination. *J. Geophys. Res.* 111(D6):D06102

Ren J, Jiang H, Seidenkrantz M-S, Kuijpers A. 2009. A diatom-based reconstruction of Early Holocene hydrographic and climatic change in a southwest Greenland fjord. *Mar. Micropaleontol.* 70:166–76

Renssen H, Seppä H, Heiri O, Roche DM, Goosse H, Fichefet T. 2009. The spatial and temporal complexity of the Holocene thermal maximum. *Nat. Geosci.* 2:411–14

Risebrobakken B, Jansen E, Andersson C, Mjelde E, Hevrøy K. 2003. A high-resolution study of Holocene paleoclimatic and paleoceanographic changes in the Nordic Seas. *Paleoceanography* 18:1017

Rosell-Melé A, McClymont EL. 2007. Biomarkers as paleoceanographic proxies. In *Proxies in Late Cenozoic Paleoceanography*, ed. C Hillaire-Marcel, A de Vernal, pp. 441–90. Amsterdam: Elsevier

Sachs JP. 2007. Cooling of Northwest Atlantic slope waters during the Holocene. *Geophys. Res. Lett.* 34:L03609

Saini J, Stein R, Fahl K, Weiser J, Hebbeln D, et al. 2020. Holocene variability in sea ice and primary productivity in the northeastern Baffin Bay. *Arktos* 6:55–73

Schmidt S, Wagner B, Heiri O, Klug M, Bennike OLE, Melles M. 2011. Chironomids as indicators of the Holocene climatic and environmental history of two lakes in Northeast Greenland. *Boreas* 40:116–30

Schweinsberg AD, Briner JP, Licciardi JM, Bennike O, Lifton NA, et al. 2019. Multiple independent records of local glacier variability on Nuussuaq, West Greenland, during the Holocene. *Quat. Sci. Rev.* 215:253–71

Schweinsberg AD, Briner JP, Miller GH, Bennike O, Thomas EK. 2017. Local glaciation in West Greenland linked to North Atlantic Ocean circulation during the Holocene. *Geology* 45:195–98

Schweinsberg AD, Briner JP, Miller GH, Lifton NA, Bennike O, Graham BL. 2018. Holocene mountain glacier history in the Sukkertoppen Iskappe area, southwest Greenland. *Quat. Sci. Rev.* 197:142–61

Seidenkrantz M-S. 2013. Benthic foraminifera as palaeo sea-ice indicators in the subarctic realm—examples from the Labrador Sea–Baffin Bay region. *Quat. Sci. Rev.* 79:135–44

Seidenkrantz M-S, Aagaard-Sorensen S, Sulsbruck H, Kuijpers A, Jensen KG, Kunzendorf H. 2007. Hydrography and climate of the last 4400 years in a SW Greenland fjord: implications for Labrador Sea palaeoceanography. *Holocene* 17:387–401

Seidenkrantz M-S, Roncaglia L, Fischel A, Heilmann-Clausen C, Kuijpers A, Moros M. 2008. Variable North Atlantic climate seesaw patterns documented by a late Holocene marine record from Disko Bugt, West Greenland. *Mar. Micropaleontol.* 68:66–83

Sejrup HP, Seppä H, McKay NP, Kaufman DS, Geirsdóttir Á, et al. 2016. North Atlantic-Fennoscandian Holocene climate trends and mechanisms. *Quat. Sci. Rev.* 147:365–78

Sha L, Jiang H, Knudsen KL. 2011. Diatom evidence of climatic change in Holsteinsborg Dyb, west of Greenland, during the last 1200 years. *Holocene* 22:347–58

Sha L, Jiang H, Seidenkrantz M-S, Knudsen KL, Olsen J, et al. 2014. A diatom-based sea-ice reconstruction for the Vaigat Strait (Disko Bugt, West Greenland) over the last 5000 yr. *Palaeogeogr. Palaeoclimatol. Palaeoecol.* 403:66–79

Sha L, Jiang H, Seidenkrantz M-S, Li D, Andresen CS, et al. 2017. A record of Holocene sea-ice variability off West Greenland and its potential forcing factors. *Palaeogeogr. Palaeoclimatol. Palaeoecol.* 475:115–24

Simpson MJR, Milne GA, Huybrechts P, Long AJ. 2009. Calibrating a glaciological model of the Greenland ice sheet from the Last Glacial Maximum to present-day using field observations of relative sea level and ice extent. *Quat. Sci. Rev.* 28:1631–57

Sinclair G, Carlson AE, Mix AC, Lecavalier BS, Milne G, et al. 2016. Diachronous retreat of the Greenland ice sheet during the last deglaciation. *Quat. Sci. Rev.* 145:243–58

Solignac S, Giraudeau J, de Vernal A. 2006. Holocene sea surface conditions in the western North Atlantic: spatial and temporal heterogeneities. *Paleoceanography* 21:PA2004

Søndergaard AS, Larsen NK, Lecavalier BS, Olsen J, Fitzpatrick NP, et al. 2020. Early Holocene collapse of marine-based ice in northwest Greenland triggered by atmospheric warming. *Quat. Sci. Rev.* 239:106360

Stammer D. 2008. Response of the global ocean to Greenland and Antarctic ice melting. *J. Geophys. Res.* 113(C6):C06022

Syring N, Stein R, Fahl K, Vahlenkamp M, Zehnich M, et al. 2020. Holocene changes in sea-ice cover and polynya formation along the eastern North Greenland shelf: new insights from biomarker records. *Quat. Sci. Rev.* 231:106173

Telford RJ, Li C, Kucera M. 2013. Mismatch between the depth habitat of planktonic foraminifera and the calibration depth of SST transfer functions may bias reconstructions. *Clim. Past* 9:859–70

Thomas EK, Briner JP, Ryan-Henry JJ, Huang YS. 2016. A major increase in winter snowfall during the middle Holocene on western Greenland caused by reduced sea ice in Baffin Bay and the Labrador Sea. *Geophys. Res. Lett.* 43:5302–8

Thomas EK, Castañeda IS, McKay NP, Briner JP, Salacup JM, et al. 2018. A wetter Arctic coincident with hemispheric warming 8,000 years ago. *Geophys. Res. Lett.* 45:10637–47

van der Bilt WGM, Rea B, Spagnolo M, Roerdink DL, Jørgensen SL, Bakke J. 2018. Novel sedimentological fingerprints link shifting depositional processes to Holocene climate transitions in East Greenland. *Glob. Planet. Change* 164:52–64

Van Nieuwenhove N, Baumann A, Matthiessen J, Bonnet S, de Vernal A. 2016. Sea surface conditions in the southern Nordic Seas during the Holocene based on dinoflagellate cyst assemblages. *Holocene* 26:722–35

Vinther BM, Buchardt SL, Clausen HB, Dahl-Jensen D, Johnsen SJ, et al. 2009. Holocene thinning of the Greenland ice sheet. *Nature* 461:385–88

Vinther BM, Clausen HB, Johnsen SJ, Rasmussen SO, Andersen KK, et al. 2006. A synchronized dating of three Greenland ice cores throughout the Holocene. *J. Geophys. Res.* 111(D13):D13102

von Gunten L, D'Andrea WJ, Bradley RS, Huang Y. 2012. Proxy-to-proxy calibration: increasing the temporal resolution of quantitative climate reconstructions. *Sci. Rep.* 2:609

Walker M, Head MJ, Berkelhammer M, Björck S, Cheng H, et al. 2018. Formal ratification of the subdivision of the Holocene Series/Epoch (Quaternary System/Period): two new Global Boundary Stratotype Sections and Points (GSSPs) and three new stages/subseries. *Episodes* 41:213–23

Weidick A, Bennike O. 2007. Quaternary glaciation history and glaciology of Jakobshavn Isbræ and the Disko Bugt region, West Greenland: a review. *Geol. Surv. Den. Greenl. Bull.* 14:1–78

Wooller MJ, Francis D, Fogel ML, Miller GH, Walker IR, Wolfe AP. 2004. Quantitative paleotemperature estimates from δ^{18}O of chironomid head capsules preserved in arctic lake sediments. *J. Paleolimnol.* 31:67–74

Young NE, Briner JP. 2015. Holocene evolution of the western Greenland Ice Sheet: assessing geophysical ice-sheet models with geological reconstructions of ice-margin change. *Quat. Sci. Rev.* 114:1–17

Young NE, Briner JP, Axford Y, Csatho B, Babonis GS, et al. 2011a. Response of a marine-terminating Greenland outlet glacier to abrupt cooling 8200 and 9300 years ago. *Geophys. Res. Lett.* 38:L24701

Young NE, Briner JP, Stewart HAM, Axford Y, Csatho B, et al. 2011b. Response of Jakobshavn Isbrae, Greenland, to Holocene climate change. *Geology* 39:131–34